Plant Biotechnology Journal

WILEY | aab SEB

RESEARCH ARTICLE OPEN ACCESS

DNA Aptamers Targeting BcSOD1: A Novel Strategy for Controlling *Botrytis cinerea* in Sustainable Agriculture

Alba López-Laguna[1,2] | Álvaro Polonio[1,2] | Lucía Jiménez-Castro[1,2] | Yandira Morales[1,2] | Alejandra Vielba-Fernández[1,2] | M. Elena Martín[3] | Víctor M. González[3] | Antonio de Vicente[1,2] | Alejandro Pérez-García[1,2] | Dolores Fernández-Ortuño[1,2]

[1]Departamento de Microbiología, Facultad de Ciencias, Universidad de Málaga, Málaga, Spain | [2]Instituto de Hortofruticultura Subtropical y Mediterránea 'La Mayora', Universidad de Málaga, Consejo Superior de Investigaciones Científicas (IHSM–UMA–CSIC), Málaga, Spain | [3]Grupo de Aptámeros, Departamento de Bioquímica-Investigación, IRYCIS-Hospital Universitario Ramón y Cajal, Madrid, Spain

Correspondence: Dolores Fernández-Ortuño (dfernandez-ortuno@uma.es)

Received: 23 January 2025 | **Revised:** 12 July 2025 | **Accepted:** 30 July 2025

Funding: This work has been funded by: AYUDAS A LA I + D + i, EN EL ÁMBITO DEL PLAN ANDALUZ DE INVESTIGACIÓN, DESARROLLO E INNOVACIÓN (PAIDI 2020). Project code: PY20_00048.

Keywords: aptamer | biofungicide | *Botrytis cinerea* | control | reactive oxygen species | superoxide dismutase

ABSTRACT

Botrytis cinerea, the necrotrophic fungus responsible for grey mould disease, is a major threat to global crop production. Control strategies mainly rely on chemical fungicides, but resistance development limits their long-term effectiveness. This study introduces, for the first time in crop protection, the use of DNA aptamers as a novel and sustainable strategy. Aptamers are short, single-stranded DNA molecules that bind specific targets with high affinity, acting like 'chemical antibodies'. Using SELEX technology, two aptamers, SOD9.14F and SOD9.26F, were designed to target BcSOD1, a superoxide dismutase enzyme essential for fungal virulence and ROS detoxification. Molecular modelling predicted that both aptamers bind within BcSOD1's catalytic pocket. Both aptamers inhibited BcSOD1 enzymatic activity (97.5%) and reduced germination (67%), fungal biomass (58%) and lesion formation (42%) in *B. cinerea*-infected tomato leaves (*Solanum lycopersicum*) and apple fruits (*Malus domestica*). Fluorescence microscopy confirmed aptamer binding to conidia surfaces. No antifungal effect was observed in the *ΔBcsod1* mutant or with the non-structured control aptamer Ap.AGA, supporting target specificity. RNA-Seq analysis revealed that SOD9.26F interfered with fungal oxidative stress responses and metabolism. Additionally, aptamer application primed tomato plants, activating defence-related gene expression. Interestingly, Ap.AGA aptamer triggered partial priming, suggesting a broader DNA-induced effect. These findings validate BcSOD1 as an antifungal target and highlight aptamers as dual-action agents: impairing fungal development and enhancing plant immunity. This study positions DNA aptamers as specific, effective and sustainable tools for integrated management of grey mould in agriculture.

1 | Introduction

Fungi are the main group of pathogens responsible for plant diseases (Doehlemann et al. 2017), with *Botrytis cinerea*, the necrotrophic fungus causing grey mould disease, being one of the most destructive. This pathogen affects over 1000 plant species, including vegetables, fruit trees and ornamental plants, resulting in significant yield losses, both pre- and post-harvest (Petrasch et al. 2019). Due to its extensive economic and agricultural impact, it ranks as the second most significant phytopathogen worldwide (Dean et al. 2012). Control strategies have heavily relied on the widespread use of commercial fungicides, but their extensive use has led to the rapid emergence of multi-resistant *B. cinerea* strains (Kim and Xiao 2011; Fernández-Ortuño

et al. 2015, 2017; Lopes et al. 2017; Sang et al. 2018; Harper et al. 2021), making alternative control strategies essential to meet consumer demand for sustainable agriculture. This adaptability of *B. cinerea* stems from its polycyclic nature and genetic diversity, which allow it to overcome fungicide pressures (Williamson et al. 2007; Choquer et al. 2007). Furthermore, its genome contains unique features, such as transposable elements and accessory chromosomes, which influence its genetic changes and adaptability (Amselem et al. 2011; Van Kan et al. 2017).

Plants naturally defend themselves against pathogens through mechanisms like the oxidative burst, which generates reactive oxygen species (ROS). ROS promote several host plant defence reactions such as a hypersensitive response (HR), which causes cell death adjacent to the pathogen penetration site, resulting in local necrosis and limiting pathogen progress (de Gara et al. 2003; Rolke et al. 2004; López-Cruz et al. 2017). To counteract oxidative damage, *B. cinerea* employs various detoxification systems, including non-enzymatic and enzymatic degradation systems, such as catalases, peroxidases and superoxide dismutases (SODs; Govrin and Levine 2000; Rolke et al. 2004; Siegmund and Viefhues 2016; López-Cruz et al. 2017). SODs are crucial metalloenzymes that dismutate the superoxide anions into less harmful products. They are classified into four types depending on the metal cofactor used: copper–zinc (Cu-ZnSOD), iron (FeSOD), manganese (MnSOD) and nickel (NiSOD) binding (Fridovich 1981; Youn et al. 1996). In *B. cinerea*, four SOD proteins have been identified (BcSOD1, BcSOD2, BcSOD3 and BcSOD4; Amselem et al. 2011; Staats and van Kan 2012; Van Kan et al. 2017), among which BcSOD1 is the major Cu/Zn-SOD. This enzyme plays a central role in ROS detoxification and is critical for the pathogenicity of *B. cinerea* (Rolke et al. 2004), making it a prime target for innovative control strategies.

Aptamers are small synthetic single-stranded DNA (ssDNA) or RNA molecules, typically 10–100 nucleotides in length, that fold into unique three-dimensional structures. This folding allows them to bind with high specificity to target molecules (Ellington and Szostak 1990; Tuerk and Gold 1990; Zou et al. 2019). Their ability to discriminate between a target molecule and its analogues or to distinguish different conformations of the same molecule makes them highly versatile (Proske et al. 2002; Ku et al. 2015). For this reason, aptamers are often referred to as 'chemical antibodies' due to their remarkable binding capabilities (Banerjee 2010; Wang, Chang, and Lee 2016). Since their discovery in the 1990s, aptamers have gained significant attention, particularly in the biotechnology and clinical sectors. They are now being used to replace antibodies in various therapeutic and diagnostic applications, thanks to their stability, scalability and cost-effectiveness (Missailidis and Hardy 2009; Wang, Chang, and Lee 2016). For instance, aptamers have been developed for use as antivirals (Gopinath et al. 2012; Huang et al. 2024), in cancer therapy (Mahlknecht et al. 2013; Ku et al. 2015) and as biosensors for biomarkers detection and molecular imaging (Shi et al. 2011; Ku et al. 2015). The agricultural and food industries have also embraced aptamers due to their potential for developing biosensors. These aptamer-based tools can detect biomolecules and pathogens with precision, offering promising applications in ensuring food safety. To date, aptamers have been successfully developed to detect allergens (Amaya-González et al. 2014), antibiotics, fertiliser residues and pesticides (He et al. 2011; Han et al. 2014; Pang et al. 2014), mycotoxins (Nguyen et al. 2013; Hernández et al. 2020) and microorganisms in food (Wang et al. 2020). The versatility and potential of aptamers in diverse fields continue to drive innovation, marking them as powerful tools for addressing critical challenges in healthcare, agriculture and beyond.

This study pioneers the use of DNA-aptamers in crop protection as revolutionary biofungicides against the phytopathogenic fungus *B. cinerea*. By specifically targeting the BcSOD1 protein, a key player in the fungus's oxidative stress response mechanism, our findings demonstrate that aptamers can significantly reduce conidial germination and disease progression in two different hosts. Moreover, RNA-Seq analyses of *B. cinerea* and tomato leaves treated with aptamers revealed the disruption of ROS detoxification in the fungus and the activation of defence signalling in the host, respectively. Our results the way for the future development of aptamer-based products as an innovative strategy for disease management, offering a promising and environmentally friendly solution to combat grey mould, one of the most devastating crop diseases worldwide.

2 | Results

2.1 | BcSOD1 Protein Was Expressed, Purified and Showed Superoxide Dismutase Activity

To develop aptamers against BcSOD1 (Figure 1a,b), the protein was expressed in vitro using *Escherichia coli* Bl21-CodonPlus-RIL cells as a 6 His-tagged fusion. BcSOD1 was predominantly present in the soluble fraction and was subsequently purified by immobilisation using a nickel affinity column (Figure 1c), yielding a protein concentration of $900\,\mu g\,mL^{-1}$. To confirm the enzymatic activity of BcSOD1, a cytochrome c reduction inhibition assay was conducted using xanthine and xanthine oxidase as sources of superoxide ions (Ghe et al. 1985). SOD enzymes compete with cytochrome c for these ions, thereby inhibiting its reduction. The rate of cytochrome c reduction was measured spectrophotometrically at 550 nm in a control system (without SOD) to observe the baseline absorbance increase ($\Delta A_{550\,nm}$) during the first minute. $\Delta A_{550\,nm}$ in the presence of increasing BcSOD1 concentrations was then analysed, and the inhibition of the cytochrome c reduction was calculated using the formula described in Section 4.3. The results showed a clear correlation between higher BcSOD1 concentrations and increased inhibition rates (Figure 1d), reaching 59% inhibition at the highest concentration tested ($5\,\mu g\,mL^{-1}$). These findings confirm that the His-tagged BcSOD1 exhibits strong superoxide dismutase activity.

2.2 | Two High-Affinity Aptamers Were Identified and Characterised That Display In Silico Binding Capabilities and Appear to Block the Catalytic Pocket of BcSOD1

The aptamers targeting the BcSOD1 protein were identified through an innovative approach known as Systematic Evolution of Ligands by Exponential Enrichment (SELEX;

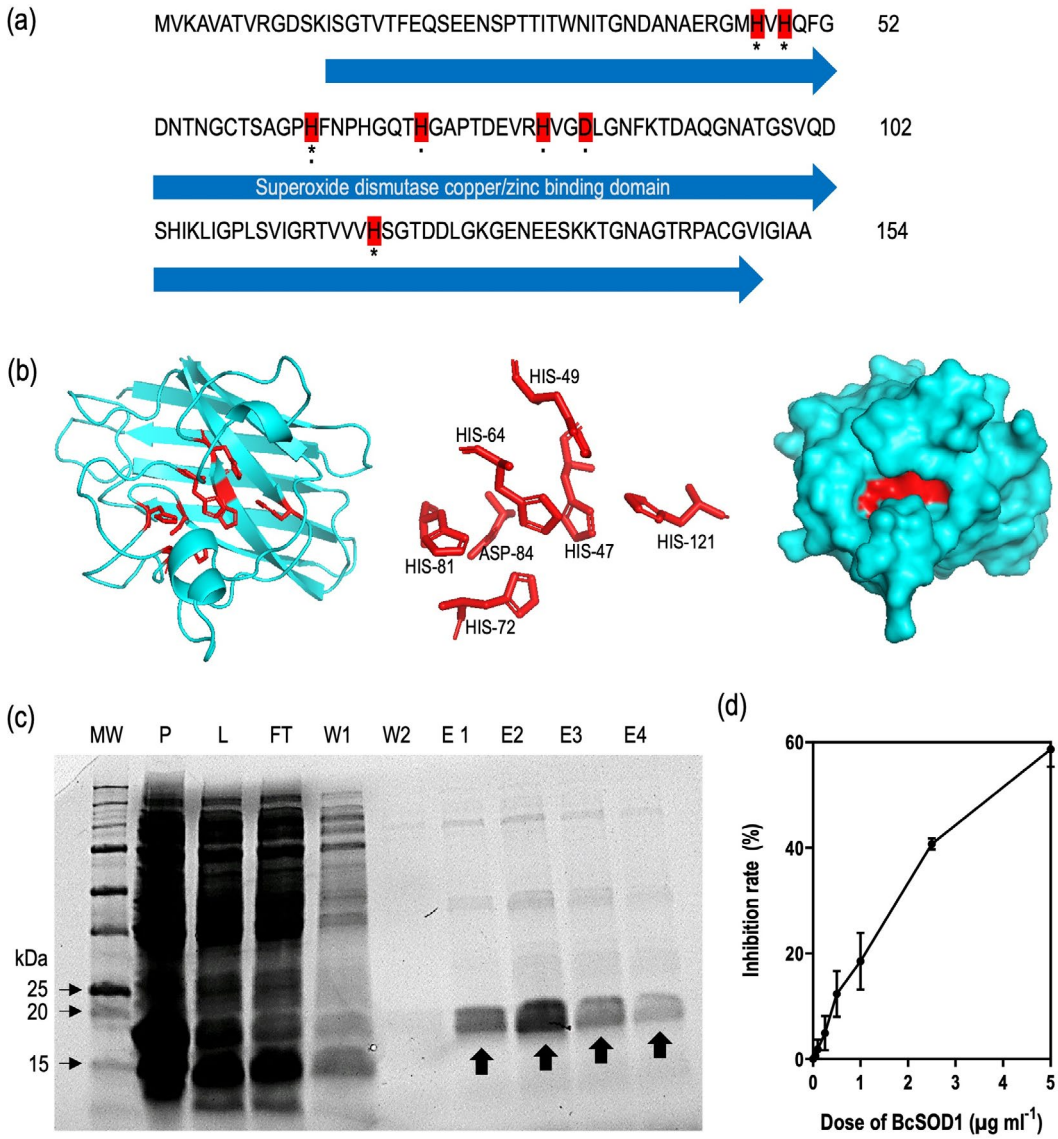

FIGURE 1 | Main features and in vitro expression of BcSOD1 protein. (a) Amino acid sequence of BcSOD1. The amino acids of the active centre are highlighted by red boxes. Copper (Cu^{2+}) and zinc (Zn^{2+}) binding sites are marked with asterisks and dots, respectively. The superoxide dismutase copper/zinc binding domain is indicated with blue arrows. (b) Three-dimensional (3D) structure of BcSOD1. The 3D model predicted by the AlphaFold server is shown. The protein structure and the active center are displayed in sky blue and red colours, respectively. These 3D structures were visualised with Pymol software. (c) In vitro expression and purification of His-tagged BcSOD1 protein. The image shows the different steps of the protein purification process, visualised using a Gel Doc XR+ (Bio-Rad) with Mini-PROTEAN TGX Precast Gel (Bio-Rad). Arrows indicate the bands corresponding to the soluble purified BcSOD1 protein. Lanes are: E1–E4, eluted soluble protein samples; FT, flow-through sample collected after protein-column binding; L, supernatant sample obtained after cell lysing; MW, protein marker Precision Plus Protein Unstained Standards (10–250 kDa; Bio-Rad); P, pellet sample; W1, first wash sample; W2, second wash sample. (d) Activity of His-tagged BcSOD1 protein. The rate of cytochrome c reduction by BcSOD1 was measured spectrophotometrically at 550 nm within 1 min. The graph represents the mean ± SEM of three technical replicates.

Figure S1; Tuerk and Gold 1990). This process was conducted at the Aptamers Laboratory of the Institute Ramón y Cajal (IRyCIS, Madrid, Spain), utilising a random ssDNA (RND40) library. Nine rounds of incubation, binding, partitioning and amplification were performed to screen for aptamers with high affinity to BcSOD1 under physiological conditions. An Enzyme-Linked Oligonucleotide Assay (ELONA) confirmed the binding potential of selected aptamer populations, narrowing the library to clones with optimal specificity and affinity. The control used consists of the secondary antibody alone, which serves to confirm that the observed signal is specifically due to the binding of the aptamer populations. Then, the signal intensity obtained across the different aptamer populations was compared. A significant enrichment was observed in R9 compared to the other rounds analysed (Figure 2a), so the cloning of this round was proceeded. Eighteen R9 clones were obtained and subsequently checked for affinity by ELONA, observing a higher affinity for the BcSOD1 protein clones 14, 19, 23, 24 and 26 (Figure 2b). These clones were sequenced, and double-stranded DNA

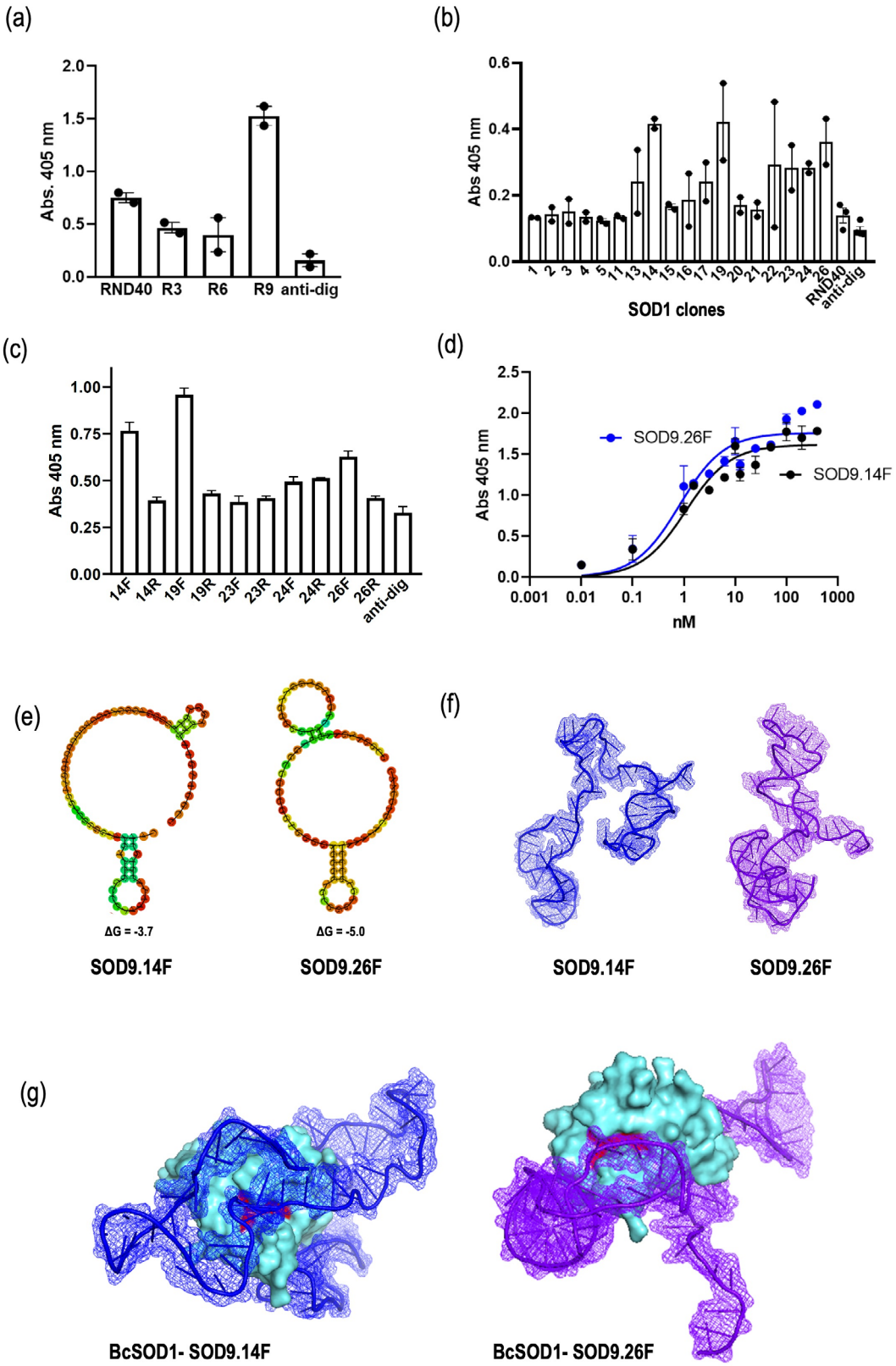

FIGURE 2 | Legend on next page.

was produced by polymerase chain reaction (PCR). Both strands (called F and R strands) were used in a further selection process. The affinity of each chain for BcSOD1 was re-evaluated using ELONA, revealing that clones 14F, 19F and 26F exhibited the highest binding, each producing a signal more than twice that of the anti-DIG control (Figure 2c; as previously described by García-Recio et al. 2016); however, sequence analysis indicated that clones 14 and 19 were the same clone. On the basis of these results, two promising candidates, SOD9.14F (5′-GCGGATGAAGACTGGTGTCGGGG

FIGURE 2 | Selection and identification of aptamers targeting BcSOD1 with SELEX technology. (a) Comparison of rounds 3 (R3), 6 (R6) and 9 (R9) aptamer populations for BcSOD1 through ELONA assay. BcSOD1 protein was incubated with digoxigenin-labelled R3, R6 and R9 aptamer populations or digoxigenin-labelled RND40. (b) Clones obtained from R9 and the initial RND40 pool were analysed using ELONA. (c) ELONA analysis of the F and R chain from selected clones with the highest affinity for BcSOD1. Graphs represent the mean ± SEM from two independent experiments. (d) Determination of the binding affinity (Kd) of aptamers to BcSOD1 using ELONA. BcSOD1 protein was incubated with digoxigenin-labelled aptamers at increasing concentrations (0–800 nM). The graphs show the mean ± SEM from three independent experiments. (e) Predicted secondary structures of aptamers SOD9.14F and SOD9.26F were obtained using RNA fold software. (f) Three-dimensional (3D) structure of SOD9.14F and SOD9.26F aptamers were modelled with 3dDNA tools software. (g) Molecular docking analysis of aptamers-BcSOD1 binding was performed using HDOCK server.

AGGGTGGGAGGGGGAGGTAGGTCGGGGTATGATCGGC CCTAAATACGAGCAAC-3′) and SOD9.26F (5′-GCGGATG AAGACTGGTGTGGTTGGGGGTCTGGCGGGGGGTGGGG AGGGCTGCGGGTGTGCCCTAAATACGAGCAAC-3′) were selected. Both exhibited strong binding capabilities with dissociation constants (Kd) of 1.09 ± 0.28 nM and 0.83 ± 0.22 nM, respectively (Figure 2d). Furthermore, the same enzymatic assay described previously validated their ability to inhibit BcSOD1 activity during the enzymatic reduction of cytochrome c in a dose-dependent manner. For this purpose, increasing concentrations (0.1, 1, 1, 10 and 100 nM) of both aptamers were incubated together with 5 μg mL^{-1} of the BcSOD1 protein at different times. BcSOD1 activity was reduced by an average of 77.4%, 97.5% and 95% after 1, 6 and 24 h incubation, respectively, at the higher concentration. In addition, the most likely secondary structure (Figure 2e) and the 3D structure (Figure 2f) of each aptamer were predicted using RNA fold and 3dDNA tools, respectively. These 3D structures were used to perform molecular modelling analysis of aptamer-BcSOD1 binding, revealing that both aptamers effectively bind BcSOD1 (Figure 2g) with high Confidence Scores (Table S2), apparently blocking the catalytic pocket of the enzyme and providing a molecular explanation for their high inhibitory activity.

2.3 | SOD9.14F and SOD9.26F Aptamers Are Localised on the Surface of Germinated Conidia of *B. cinerea*

To confirm the binding of SOD9.14F and SOD9.26F aptamers to BcSOD1 in *B. cinerea*, conidia of the wild-type strain B05.10 were treated with 50 μM fluorescein-labelled aptamers. Unlabeled aptamers and Milli-Q water served as negative controls. Following treatment, micrococcal nuclease digestion was applied to degrade unbound aptamers. After 9 h of incubation, confocal microscopy revealed strong fluorescence localised to the surface of germinated conidia treated with labelled aptamers, while no signal was detected in the control treatments (Figure 3). Binding specificity was further validated using the Δ*Bcsod1* mutant, which showed a drastic reduction in surface fluorescence, though a faint residual signal persisted (Figure 3). This weak residual signal suggested potential off-target interactions, prompting further analysis of other *B. cinerea* SOD proteins. Among the four SOD genes in *B. cinerea* (*Bcsod1*: Bcin03g03390, *Bcsod2*: Bcin06g03160, *Bcsod3*: Bcin01g03830 and *Bcsod4*: Bcin05g05040), only BcSOD2 protein displayed features compatible with extracellular localization and structural similarity to BcSOD1. Specifically, DeepLoc-2.0 (Almagro-Armenteros et al. 2017) predicted BcSOD2 as an extracellular protein (localization probability = 0.7325) with Gene Ontology (GO) terms associated with 'extracellular region' (GO:0005576), 'cell surface' (GO:0009986) and 'fungal-type cell wall' (GO:0009277) according with CATH/Gene 3D (Sillitoe et al. 2021). In addition, BcSOD2 contains a GPI-anchor domain that could mediate limited membrane localization (Pierleoni et al. 2008). Despite these features, sequence identity between *Bcsod1* and *Bcsod2* is low (17.44%), and molecular docking simulations showed that while aptamers SOD9.14F and SOD9.26F can bind BcSOD2, neither is predicted to block its active site (Figure S2; Table S2), indicating non-inhibitory binding as it was the case of BcSOD1 (Figure 2g). In contrast, BcSOD3 and BcSOD4 are both predicted mitochondrial proteins by Deep-Loc-2.0 (localization probabilities 0.9242 and 0.8450, respectively), each containing mitochondrial transit peptides and thus unlikely to be accessible during plant infection. Taken together, these findings indicate that the limited fluorescence observed in the Δ*Bcsod1* mutant likely results from weak, non-functional interaction with BcSOD2, confirming BcSOD1 as the primary and most effective target for aptamer-based antifungal intervention. In addition, the results are further supported by the germination assays described below, which reinforce the target specificity and functional relevance of BcSOD1 in early fungal development.

2.4 | Aptamers Targeting BcSOD1 Inhibit *B. cinerea* Germination

To investigate the inhibitory effect of SOD9.14F and SOD9.26F aptamers on *B. cinerea* conidia germination, an in vitro assay was performed. Fungal conidia from both the wild-type strain B05.10 and the Δ*Bcsod1* mutant were treated with increasing concentrations of aptamers (50, 100 and 200 μM) on 2% water-agar medium in 12-well plates. Milli-Q water, the control aptamer Ap.AGA, and a commercial fungicide (fludioxonil, Geoxe) at a sublethal dose (10 μM) were used as negative and positive controls, respectively. After 9 h of incubation, light microscopy revealed a marked reduction in conidial germination in wild-type samples treated with SOD9.14F and SOD9.26F, whereas no inhibitory effect was observed in the Δ*Bcsod1* mutant (Figure 4a). Germination rate was quantified by comparing the germination tube length of conidia in treated samples relative to water-treated controls. In the wild-type strain, both aptamers significantly reduced germination in a dose-dependent manner, with inhibition ranging from ~35% at 50 μM to ~65% at 200 μM (Figure 4b). In contrast, the Δ*Bcsod1* mutant remained largely unaffected by either aptamer treatment at all concentrations tested. The control aptamer Ap.AGA showed no inhibitory effect on germination in either strain. These results indicate that

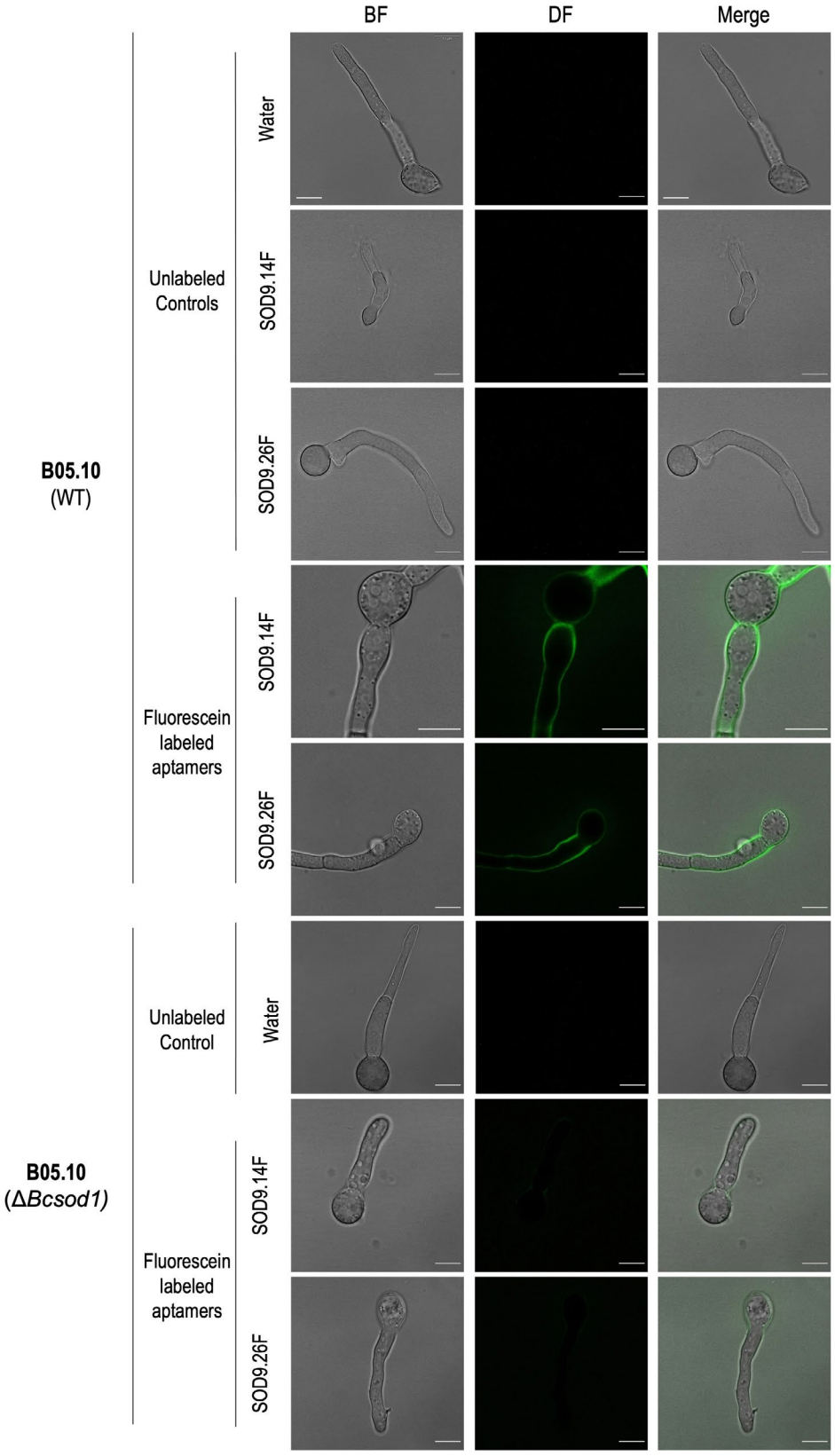

FIGURE 3 | Localization of SOD9.14F and SOD9.26F aptamers on the surface of *Botrytis cinerea* germinated conidia. Confocal laser scanning microscopy (CLSM) images of germinated spores 9 h after fluorescein-labelled aptamer treatments or control treatments (distilled water and unlabeled aptamers). Bright-field (BF), dark-field (DF) and merged images are shown. Strong surface fluorescence was observed in *B. cinerea* B05.10 strain (WT) conidia treated with both labelled aptamers, whereas no signal was detected in controls. In the Δ*Bcsod1* mutant, fluorescence was drastically reduced, although a faint signal was occasionally observed. Scale bar = 10 μm.

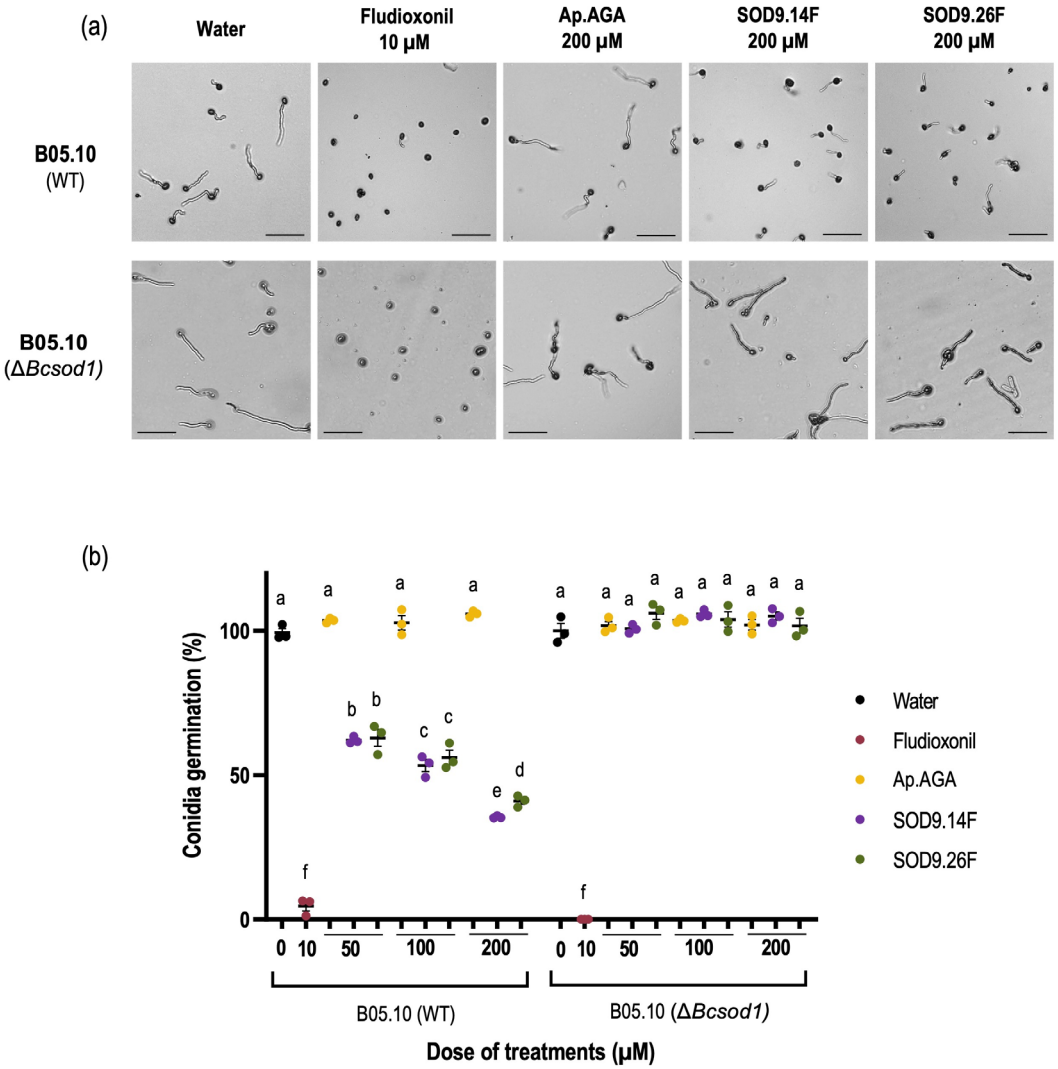

FIGURE 4 | Aptamers SOD9.14F and SOD9.26F reduce *Botrytis cinerea* conidia germination in a BcSOD1-dependent manner. (a) Representative light microscopy images (10× magnification) of *B. cinerea* conidia germination after 9 h of incubation on 2% water–agar medium supplemented with different treatments. Conidia from wild-type (WT) strain B05.10 and the Δ*Bcsod1* mutant were treated with Milli-Q water (negative control), the fungicide fludioxonil (10 µM, positive control), the control DNA aptamer Ap.AGA (50, 100 and 200 µM) or the aptamers SOD9.14F and SOD9.26F (50, 100 and 200 µM). A reduction in germination is observed in WT conidia treated with both SOD aptamers, while Δ*Bcsod1* mutant conidia remain unaffected. Scale bar = 100 µm. (b) Quantification of conidial germination percentage based on germ tube emergence using ImageJ software. Values represent mean ± SEM of 360 conidia measured from three independent experiments. Different letters indicate statistically significant differences between treatments ($p \leq 0.05$; Fisher's least significant difference test, LSD).

the inhibitory effect of SOD9.14F and SOD9.26F is dependent on the presence of BcSOD1, supporting the specificity of aptamer–target interaction.

2.5 | Topical Application of Aptamers on Detached Tomato Leaves and Apple Fruit Reduces the Development of *B. cinerea*

The efficacy of SOD9.14F and SOD9.26F aptamers in controlling *B. cinerea* was evaluated on detached tomato leaves and apple fruit sprayed with SOD9.14F and SOD9.26F aptamer solutions at different concentrations, followed by inoculation with *B. cinerea*. In the case of tomato leaves, these were sprayed with aptamer solutions at 50, 100 and 200 µM. Leaves treated with the negative control (sterile distilled water) exhibited a 90% necrotic area, indicating a successful fungal infection. In contrast, leaves treated with both aptamers showed significantly reduced necrotic areas, with the reduction correlating to the aptamer concentration applied (Figure 5a,b). Compared to the negative control, the lesion size reduction was 34% in leaves treated with the aptamers at 50 µM (31% and 38% for the aptamers SOD9.14F and SOD9.26F, respectively), 33% at 100 µM (30% and 36% for SOD9.14F and SOD9.26F aptamers, respectively) and 42% at 200 µM (46% and 38% for SOD9.14F and SOD9.26F aptamers, respectively). Statistical analysis confirmed that lesion size reduction was significantly greater at 200 µM compared to lower concentrations for SOD9.14F, while no significant differences were found between concentrations for SOD9.26F. Furthermore, leaves treated with the commercial fungicide Geoxe (fludioxonil field dose 1000 µM) achieved a 100% reduction in necrotic lesions, demonstrating its efficacy as a positive

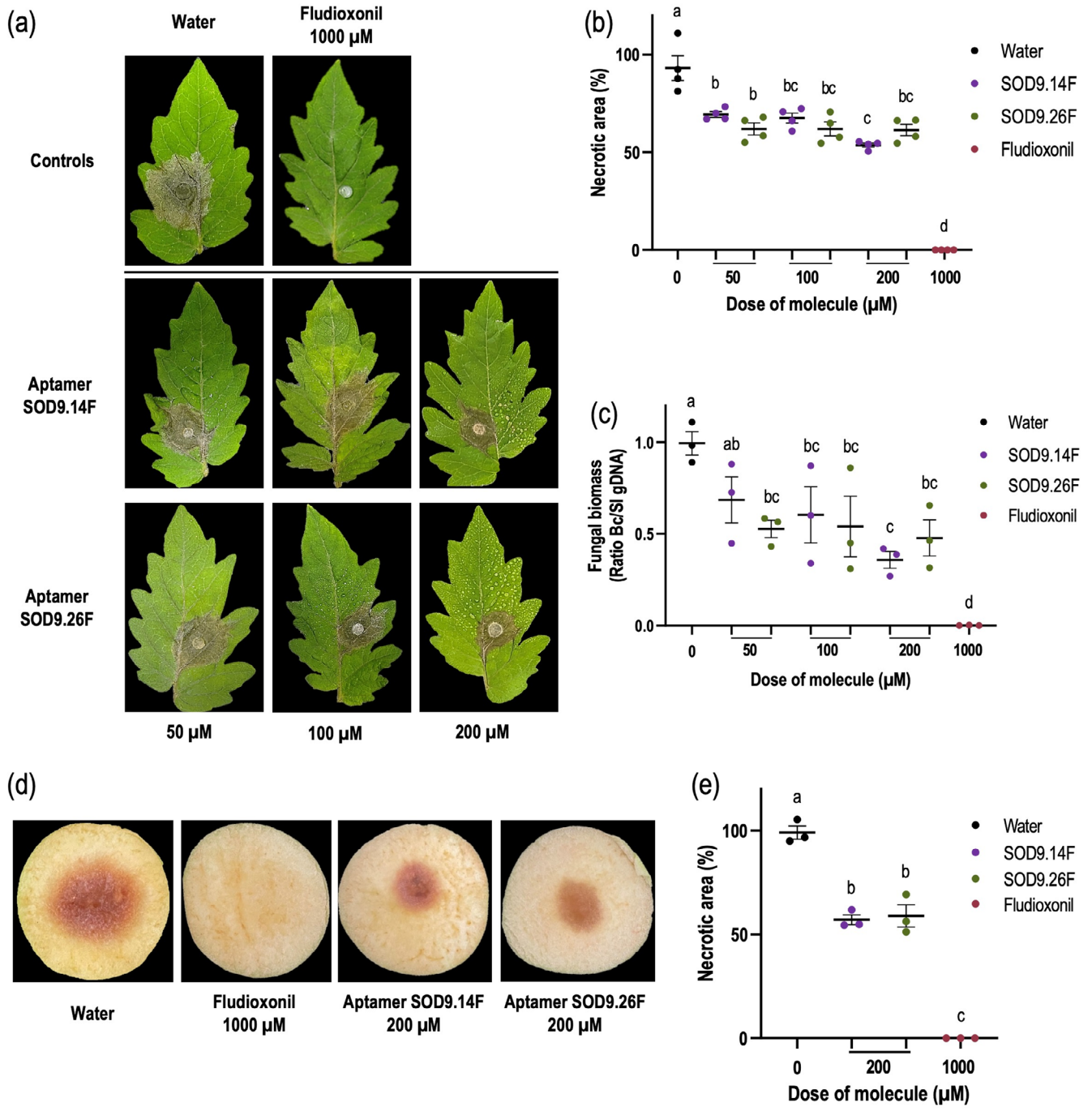

FIGURE 5 | Control effect of aptamers on grey mould disease. (a) Detached tomato leaves were treated with aptamers (50, 100, 200 µM), sterile distilled water (negative control) or 1000 µM fludioxonil (positive control) and inoculated with a PDA disc previously inoculated with *B. cinerea* conidia. (b) Necrotic areas (%) were quantified at 72 hpi using ImageJ. (c) *B. cinerea* biomass in tomato leaves treated with SOD9.14F and SOD9.26F was assessed by qPCR at 72 hpi, expressed as Bc/Sl gDNA ratio. (d) Apple fruit surfaces were treated with 200 µM aptamers, distilled water or fludioxonil and inoculated with *B. cinerea*. (e) Percentage of necrotic areas were quantified at 4 dpi using ImageJ software. Data represent mean ± SEM ($n = 15$) from three independent experiments. Equal letters indicate no statistically significant difference between treatments ($p \leq 0.05$, Fisher's LSD test).

control (Figure 5a,b). To further explore these findings, the fungal biomass on tomato leaves was analysed by qPCR. The results revealed that SOD9.14F significantly reduced fungal biomass only at concentrations of 100 and 200 µM, causing 40% and 64% reductions compared with the negative control (Figure 5c). In contrast, SOD9.26F achieved a 47%, 45% and 52% biomass reduction across all tested concentrations. No significant differences were observed between the three tested concentrations of this aptamer. These findings suggest that both aptamers effectively mitigate fungal development, with SOD9.14F being particularly effective at higher concentrations.

A similar test was conducted on apple fruit to assess the aptamer's ability to control *B. cinerea*. The surface of the fruit was cut lengthwise, then sprayed with 200 µM aptamer solution (the most effective concentration determined previously), inoculated

with *B. cinerea* and incubated for 4 days. The necrotic area was measured and compared with negative (sterile distilled water) and positive (Geoxe fungicide) controls. The results were similar to those previously observed in tomato leaves. Apples treated with SOD9.14F and SOD9.26F aptamers exhibited significantly smaller necrotic lesions (43% and 41% lesion size reduction, respectively) compared to the negative control (Figure 5d,e). As expected, apple fruits treated with the fungicide at the recommended field dose achieved a 100% reduction in necrotic lesions (Figure 5d,e).

2.6 | RNA-Seq Analysis Highlights the Impact of Aptamers on *B. cinerea* ROS Response and Suggest Priming Effects in Tomato Plants

To unravel the molecular mechanisms behind the inhibition of *B. cinerea* development and its impact on tomato plant physiology, RNA-Seq analyses were conducted. The experiments focused on evaluating changes in gene expression in both the fungus and the host plant, separately. For this purpose, the *B. cinerea* isolate B05.10 was incubated in PDB (containing 7.5 mM paraquat) without and with 50 μM of the aptamer SOD9.26F for 6 h under pre-established conditions (Figure S3). Simultaneously, tomato plants were treated without and with the same concentration of the SOD9.26F aptamer or the control aptamer Ap.AGA and incubated for 72 h. Total RNA was extracted from three biological replicates of each treatment, and cDNA libraries were generated and sequenced using Illumina technology. Differential gene expression (DEGs) was analysed by comparing *B. cinerea* and tomato plants treated with aptamers to their untreated controls; after normalisation of the raw reads using the median-of-ratios approach, that is, calculating the geometric mean of each gene across all samples, dividing every sample's counts by this mean to derive gene-wise ratios and taking the median of these ratios as a size factor to scale the counts. Genes with a $\log_2$ Fold Change (FC) > 1 or < −1 and an adjusted *p*-value (*padjust*) < 0.05 were selected for further analysis as a gene enrichment analysis focused on Molecular Functions terms and KEGG pathways using DAVID software (Figures 6 and 7, Figure S4; Table S3).

In the case of *B. cinerea*, 2227 genes were found to be deregulated out of a total of 11 385 genes, with 1250 genes differentially overexpressed (10.3%) and 977 genes differentially repressed (8%) (Figure 6a,b). GO enrichment analysis revealed significant alterations in molecular functions associated with highlighted oxidative stress response, such as NAD(P)-dependent oxidoreductase activity (GO:0016616, GO:0016491), NADPH dehydrogenase activity (GO:0003959) and flavoprotein dehydrogenase activity (GO:0004174), as well as iron/heme binding (GO:0005506, GO:0020037), transmembrane transport (GO:0022857, GO:0015171) and ribosomal biogenesis (Figure 6c). All these terms reflect disruptions in key fungal metabolic pathways such as glutathione metabolism (bfu00480), ribosome biogenesis (bfu03008, bfu03010) and ABC transporters (bfu02010), among others (Figure 6d). Notably, several affected pathways are linked to fungal virulence, such as tryptophan metabolism (bfu00380) involved in phytotoxins synthesis; lipid-related pathways (bfu00561, bfu01212, bfu00061), linked to membrane remodelling and effector secretion; and secondary metabolites (bfu01110), supporting toxin production and export via ABC transporters (bfu02010). The observed transcriptional reprogramming underscores the ability of SOD9.26F to disrupt critical processes underpinning oxidative stress management and pathogenicity in *B. cinerea*.

In *S. lycopersicum*, treatment with the SOD9.26F aptamer led to differential expression of 4066 genes, with 1880 upregulated (5.2%) and 2186 downregulated (6.1%) compared to untreated plants (Figure 7a,b). GO enrichment analysis identified terms related to immune signalling, including DNA-binding transcription factor activity (GO:0003700), protein kinase activity (GO:0004672), cis-regulatory region binding (GO:0000976) and signalling receptor activity (GO:0038023) (Figure 7c). These changes were associated with enriched metabolic pathways involved in plant defence, such as plant–pathogen interaction (sly04626), MAPK signalling (sly04016) and hormone signal transduction (sly04075) (Figure 7d). Interestingly, a similar transcriptional shift was observed in plants treated with the DNA control aptamer Ap.AGA, which induced expression changes in 8404 genes (5172 upregulated and 3232 downregulated) (Figure S4a,b), with overlapping enriched GO terms and KEGG pathways (Figure S4c,d). These results suggest that the application of DNA molecules, regardless of sequence specificity, can partially prime plant immune responses. To evaluate this effect, a detached tomato leaf assay was conducted following the protocol described in Section 4.7.2. Leaves were sprayed with either the control aptamer Ap.AGA (50 μM, matching the concentration used in the RNA-Seq analysis), sterile distilled water (negative control) or the specific aptamer SOD9.26F (50 μM, positive control). After treatment, all leaves were inoculated with PDA discs pre-inoculated with *B. cinerea* conidia. Following 72 h of incubation, leaves treated with Ap.AGA showed a slight (5%) reduction in grey mould symptoms (Figure S5), although this difference was not statistically significant compared to the water control (Figure S5). In contrast, SOD9.26F-treated leaves displayed a significant 26% reduction in disease severity, consistent with previous results. These findings indicate that while exogenous DNA aptamers like Ap.AGA may induce a mild priming effect on plant immunity, effective disease control is clearly sequence- and target-dependent.

Importantly, neither treatment affected the expression of genes related to redox homeostasis or oxidative stress, suggesting that plant SOD activity was not disrupted. To confirm this, molecular docking simulations were performed to evaluate the interaction of SOD9.14F and SOD9.26F with the tomato SOD1 homologue. While both aptamers showed potential binding to the plant SOD1 structure, neither was predicted to interact with its active site (Figure S6; Table S2), indicating that functional inhibition is unlikely to occur.

3 | Discussion

This research highlights the potential use of aptamer-based products as environmentally sustainable biofungicides and their integration into *B. cinerea* management programmes. Our results provide compelling evidence that aptamer-based inhibition of BcSOD1 represents a promising and specific strategy to reduce *B. cinerea* development and virulence. BcSOD1 has been shown to play a key role in ROS detoxification and

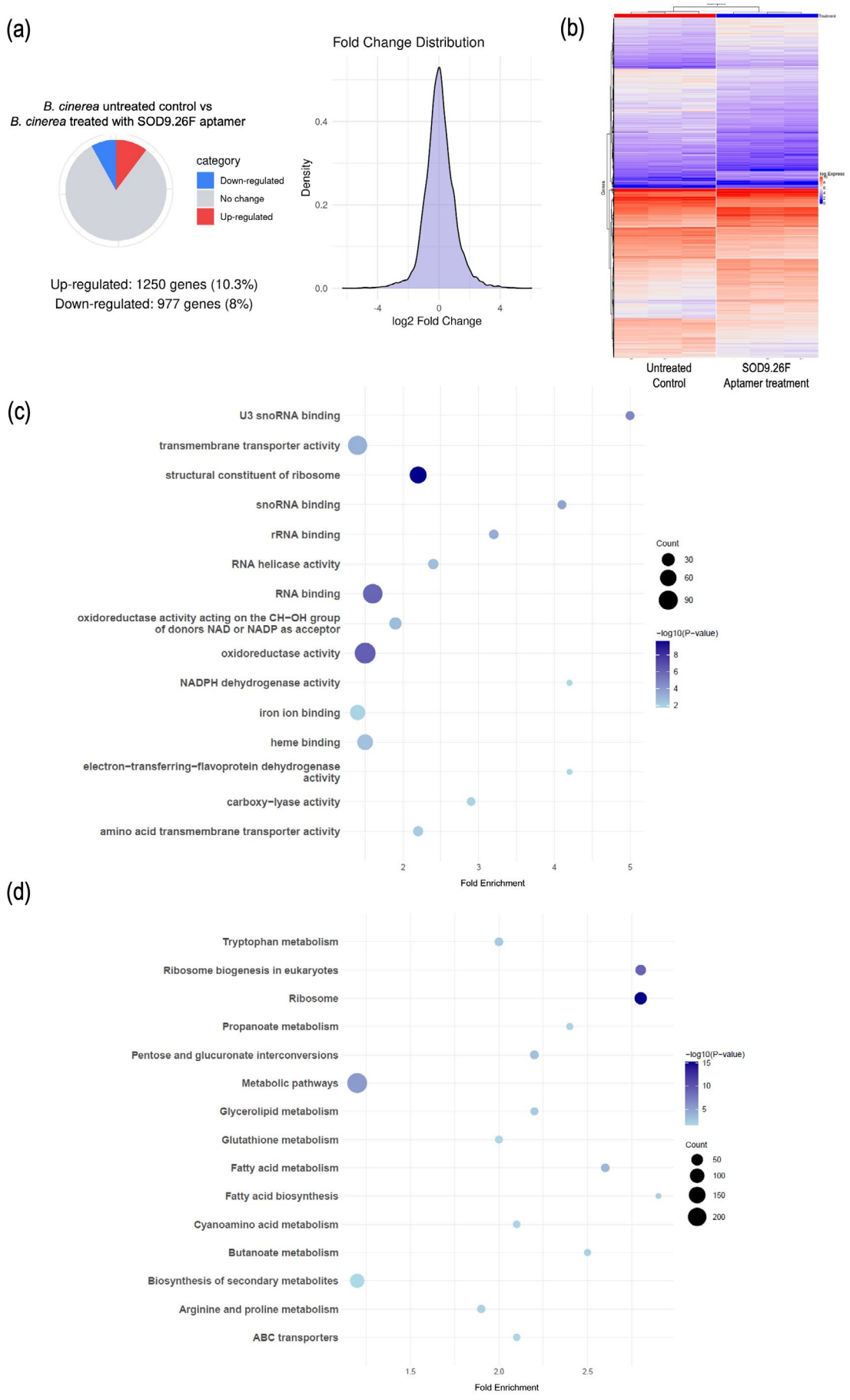

FIGURE 6 | Legend on next page.

FIGURE 6 | RNA-Seq analysis of differentially expressed genes (DEGs) in *B. cinerea* grown in PDB in the presence of paraquat (a superoxide-generating compound), not treated or treated with SOD9.26F aptamer. (a) Significant DEGs ($-1 > \text{Log}_2\ \text{FC} > 1$, and *p-adjust* < 0.05) are visualised in a pie chart: Red (upregulated), blue (downregulated) and grey (non-differentially expressed genes) genes. (b) Hierarchical clustering of *B. cinerea* gene expression (rows) after treatment with and without aptamer. Three replicates per condition (columns) were clustered using distance and average linkage. Gene expression levels are shown in a heatmap, ranging from blue (low) to red (high). (c, d) Top 15 molecular function and KEGG pathway Gene Ontology (GO) terms calculated by gene enrichment analysis of DEGs after treatment of *B. cinerea* with aptamer compared to control conditions (no aptamer treatment). (c) DEGs enrichment analysis according to their molecular functions. (d) DEGs analysis according to KEGG pathway mainly affected. Functional enrichment analysis was performed by DAVID software using those significantly DEGs ($-1 > \text{Log}_2\ \text{FC} > 1$, and *p-adjust* < 0.05) for annotation and the proteome of *B. cinerea* as background. The number of DEGs are shown as different size circles depending on the number of genes involved in each term. The colour of the circle indicates the $-\log_{10}$ *p*-value.

fungal development, including spore germination and hyphal elongation. Supporting the critical role of SOD1 in early fungal development, studies in *Schizosaccharomyces pombe* have shown that loss of SOD1 activity results in failure to proceed beyond the outgrowth stage of germination, emphasising the importance of this enzyme during spore germination and germ tube elongation (Plante et al. 2017). Deletion of *sod1* in *Fusarium graminearum* delayed hyphal and germ tube growth (Yao et al. 2016), while in *Sclerotinia sclerotiorum*, it impaired hyphae and sclerotia development (Veluchamy et al. 2012). In relation to virulence, gene silencing or knockout of *Bcsod1* leads to reduced growth of *B. cinerea* under oxidative stress and decreased virulence on hosts such as French bean, *Arabidopsis thaliana* and tomato (Rolke et al. 2004; Patel et al. 2008; López-Cruz et al. 2017). Likewise, deletion of *sod1* in *F. graminearum* reduced virulence on wheat and decreased mycotoxin production (Yao et al. 2016); in *S. sclerotiorum*, it reduced infection on tomato and tobacco (Veluchamy et al. 2012); and in *F. oxysporum* and *Verticillium dahliae*, deletion of extracellular SOD genes led to reduced colonisation and virulence in cotton and *Nicotiana benthamiana*, with increased ROS accumulation in host tissues (Wang et al. 2021; Tian, Huang, et al. 2021; Tian, Li, et al. 2021).

To functionally validate BcSOD1 as a molecular target, the activity of SOD9.14F and SOD9.26F aptamers, specifically designed to bind BcSOD1, was evaluated. These aptamers significantly inhibited conidial germination, germ tube elongation and disease progression in tomato and apple. Notably, when applied to the *ΔBcsod1* mutant, the aptamers had no effect on spore germination or germ tube elongation at any of the concentrations tested, strongly suggesting that their antifungal activity depends on the presence of the target. Furthermore, the DNA control aptamer Ap.AGA showed no inhibitory effect on either wild-type or mutant strains, confirming the sequence specificity of the SOD9.14F and SOD9.26F aptamers. This functional overlap between aptamer treatment and genetic deletion reinforces the essential role of BcSOD1 in fungal development and validates it as a precise and effective molecular target for sustainable *B. cinerea* control strategies.

Although our findings strongly support BcSOD1 as the primary functional target, demonstrated by strong aptamer binding in the wild-type strain and a marked reduction in the *ΔBcsod1* mutant, its subcellular localization remains somewhat ambiguous. Previous studies have suggested BcSOD1 as a membrane- or cell wall-associated protein secreted via an unconventional pathway, while other reports indicate predominant cytoplasmic localization (Rolke et al. 2004; Cruz-Garcia et al. 2017; Leisen et al. 2020). In some fungi, there is evidence for its extracellular (or cell wall-bound) localization, e.g., in *Aspergillus fumigatus* (Hamilton et al. 1996) and in *Claviceps purpurea* (Moore et al. 2002). In our experiments, there was no evidence that the aptamers accessed intracellular compartments, suggesting their activity may be limited to extracellular or membrane-associated pools of BcSOD1. This raises important questions about whether interaction with the secreted fraction of BcSOD1 alone accounts for the observed antifungal activity. To overcome these limitations and extend the range of accessible targets, nanocarrier systems have emerged as promising tools to promote intracellular delivery. Several studies have demonstrated the effectiveness of such systems in *B. cinerea*. Qiao et al. (2023) described the use of artificial vesicles (AVs) that significantly enhance the uptake of double-stranded RNA (dsRNA) molecules by the fungus. Similarly, Islam et al. (2021) showed that *E. coli*-derived minicells efficiently deliver gene-targeting dsRNA, resulting in complete inhibition of fungal growth and disease development in strawberry fruit, far surpassing the efficacy of unencapsulated dsRNA. Furthermore, De Angelis et al. (2022) demonstrated enhanced antifungal activity of both pterostilbene (a natural compound) and fluopyram (a synthetic fungicide) when conjugated with poly (lactic-co-glycolic acid) (PLGA) nanoparticles, which penetrated fungal conidia and hyphae within 10 min of application. These studies support the feasibility of designing aptamer-functionalized nanoparticles capable of accessing cytoplasmic targets and extending the utility of aptamer-based approaches beyond surface-localised fungal components.

Microorganisms tightly regulate the production and scavenging of reactive oxygen species (ROS) to maintain redox homeostasis, as excessive ROS can damage DNA, proteins and lipids, ultimately impairing cellular function and viability (Qin et al. 2011; Zhang et al. 2020). To mitigate oxidative stress, fungal pathogens such as *B. cinerea* rely on both enzymatic and non-enzymatic antioxidant systems, including SODs, catalases, peroxidases, the thioredoxin system and glutathione metabolism (Siegmund and Viefhues 2016). In this study, the impact of the SOD9.26F aptamer on the redox metabolism of *B. cinerea* by targeting BcSOD1 was evaluated. RNA-Seq analysis under oxidative stress conditions revealed that aptamer treatment significantly altered the expression of genes associated with ROS detoxification. Functional enrichment identified downregulation of glutathione metabolism and multiple oxidoreductase activities (e.g., NAD/NADP-dependent

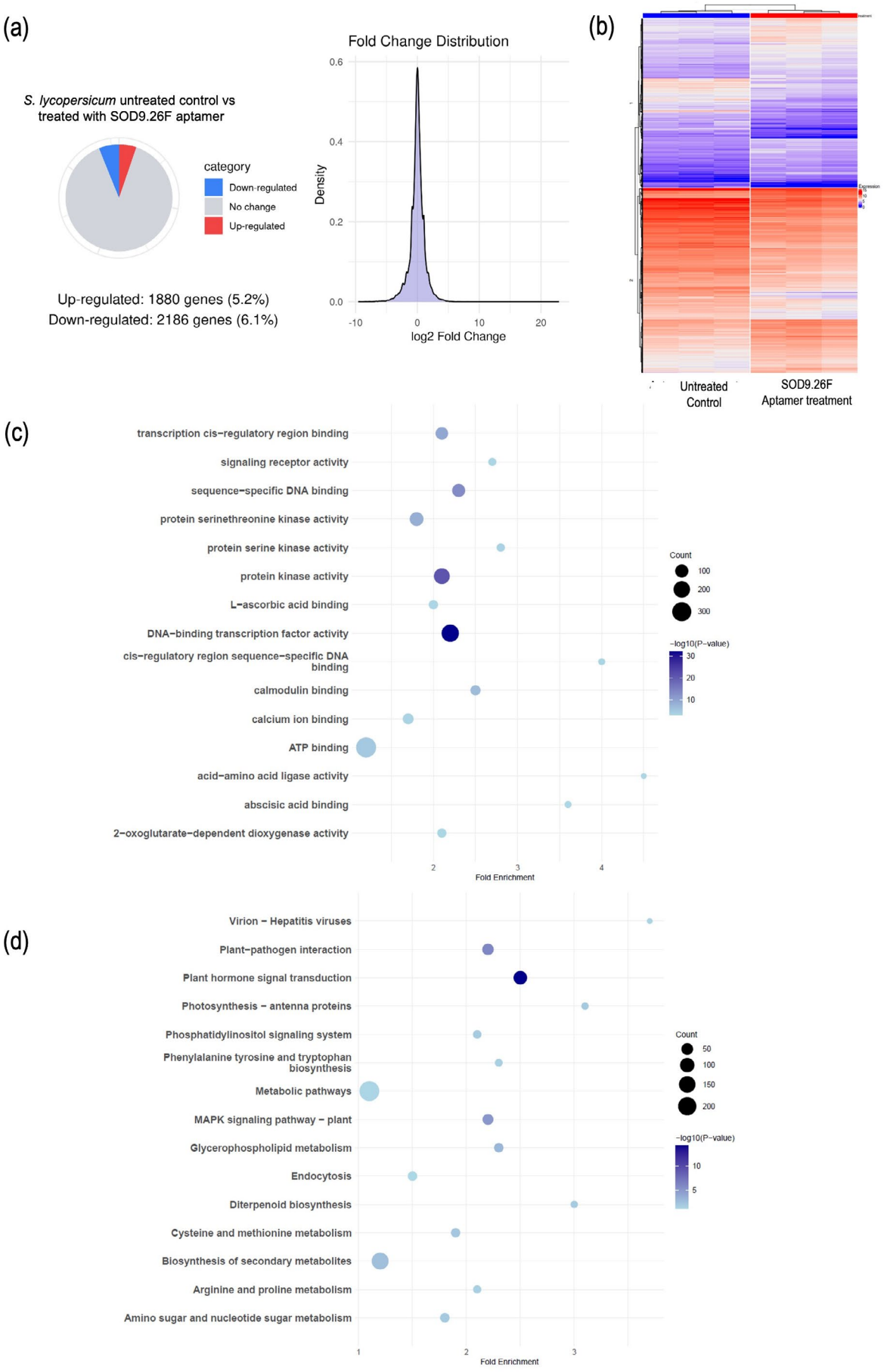

FIGURE 7 | Legend on next page.

FIGURE 7 | RNA-Seq analysis of DEGs in tomato plants (*S. lycopersicum*) not treated or treated with SOD9.26F aptamer. (a) Significant DEGs ($-1 > \text{Log}_2\ FC > 1$, and *p-adjust* < 0.05) are visualised in a pie chart: Red (upregulated), blue (downregulated) and grey (non-differentially expressed genes). (b) Hierarchical clustering of *S. lycopersicum* gene expression (rows) after treatment with and without aptamer. Three replicates per condition (columns) were clustered using distance and average linkage. Gene expression levels are shown in a heatmap, ranging from blue (low) to red (high). (c, d) Top 15 molecular function and KEGG pathway Gene Ontology (GO) terms determinate by gene enrichment analysis of DEGs after treatment of *S. lycopersicum* with aptamer compared to control without aptamer. (c) DEGs enrichment analysis depending on their molecular functions. (d) DEGs analysis based on KEGG pathway primarily impacted. DAVID software was used to perform functional enrichment analysis with those significantly DEGs ($-1 > \text{Log}_2\ FC > 1$, and *p*-adjust < 0.05) for annotation and the proteome of *S. lycopersicum* as background. The number of DEGs are represented as different size circles according to the number of genes involved in each term. The colour of the circle indicates the $-\log_{10}$ *p*-value.

dehydrogenases), as well as terms linked to FAD, heme and iron binding—critical cofactors for ROS-managing enzymes (Sellés-Vidal et al. 2018; Trisolini et al. 2019). Additionally, deregulation of pathways related to transmembrane transport, RNA processing and ribosome biogenesis suggests widespread oxidative damage (Willi et al. 2018). Together, these results indicate that SOD9.26F-mediated inhibition of BcSOD1 disrupts ROS homeostasis, leading to accumulation of oxidative stress and impaired fungal viability.

In parallel, transcriptomic profiling of *S. lycopersicum* treated with the SOD9.26F aptamer revealed the activation of immune-related signalling networks. Enriched pathways included plant hormone signal transduction, MAPK cascades and plant–pathogen interactions (Ali et al. 2022; Kaleh et al. 2024), alongside enhanced biosynthesis of defence-associated secondary metabolites and aromatic amino acids (Tzin and Galili 2010). These transcriptional changes suggest that the aptamer not only impairs fungal virulence but also primes host immunity. Interestingly, a comparable transcriptional reprogramming was observed in plants treated with the DNA control aptamer Ap.AGA, despite its lack of antifungal activity. This indicates that structured DNA molecules, regardless of sequence specificity, may act as elicitors of basal plant defence. The concept that nucleic acids can function as immune triggers is supported by previous studies (Yakushiji et al. 2009; Niehl et al. 2016; Ferrusquía-Jiménez et al. 2021; Serrano-Jamaica et al. 2021; Vega-Muñoz et al. 2023; Zhou et al. 2023). Thus, aptamers may serve a dual role: acting as highly specific inhibitors of fungal targets while also functioning to enhance host immune preparedness (Nair et al. 2022).

In summary, our results demonstrate the potential of aptamers as an environmentally friendly alternative to chemical fungicides; these biofungicides offer promising integration into sustainable crop protection programmes. Beyond aptamers, the growing success of other nucleic acid-based technologies, such as dsRNAs that harness RNA interference (RNAi), further supports the potential of oligonucleotide-based strategies. Notably, spray-induced gene silencing (SIGS) has emerged as a powerful method for controlling fungal pathogens, including *B. cinerea* (Wang, Weiberg, et al. 2016; Spada et al. 2021, 2023; Duanis-Assaf et al. 2022). Nanoparticle-mediated delivery could further enhance aptamer stability, uptake and intracellular targeting, potentially increasing their inhibitory action. These advancements collectively highlight the transformative potential of oligonucleotide molecules in developing safe, effective and eco-friendly solutions for plant disease management.

4 | Experimental Procedures

4.1 | Crops, Microbes and Culture Conditions

Apple fruit (*Malus domestica*) cv. Golden (Lleida, Spain) and tomato plants (*Solanum lycopersicum*) cv. Moneymaker (Finca Experimental 'La Mayora', Málaga, Spain) were used for in vivo assays. Plants were cultivated in growth chambers at 25°C, with 60% relative humidity, under a 16 h light/8 h dark photoperiod to ensure optimal growth conditions.

The reference strain *B. cinerea* B05.10 and the Δ*Bcsod1* mutant (kindly provided by Professor Matthias Hahn, University of Kaiserslautern-Landau) were routinely grown on potato dextrose agar (PDA) medium at 23°C, following a 16 h light/8 h dark cycle, for 7–10 days. For maintenance and genetic manipulations, the *E. coli* strain DH5α was employed, while protein expression experiments used *E. coli* BL21-CodonPlus-RIL, both cultured in lysogeny broth (LB) medium with 50 μg mL^{-1} kanamycin at 37°C.

4.2 | Isolation of Nucleic Acids and cDNA Synthesis

To extract RNA from *B. cinerea*, 3 days old colonies grown in potato dextrose broth (PDB) were harvested. Mycelium was collected, snap-frozen in liquid nitrogen and ground into powder using a mortar and pestle. Similarly, DNA from *B. cinerea*-infected tomato leaves and RNA from tomato leaves sprayed with aptamer SOD9.26F were collected for fungal biomass and gene expression studies. Genomic DNA was purified using the MasterPure Yeast DNA Purification Kit (LGC Biosearch Technologies, Teddington, Middlesex, GB), while total RNA was isolated with TRI Reagent (Sigma-Aldrich, Steinheim, Germany) according to the manufacturer's protocols. To eliminate DNA contamination, RNA samples were treated with TURBO DNAase (Thermo Fisher Scientific, Waltham, US). The quality and concentration of nucleic acids were assessed using a NanoDrop OneC UV–Vis spectrophotometer (Thermo Fisher Scientific) measuring absorbance ratios (260 nm/280 nm and 260 nm/230 nm). cDNA was synthesised using the Superscript III reverse transcriptase system (Thermo Fisher Scientific)

following the manufacturer's instructions. The samples were stored at −80°C until further analysis.

4.3 | In Vitro Production of Aptamers

4.3.1 | Construction of the Protein BcSOD1 Expression Vector

For the heterologous expression of the BcSOD1 protein (UniProtKB: A0A384JBV7), the complete open reading frame (ORF) was amplified using specific primers (listed in Table S1) designed to include *NdeI* and *XhoI* restriction sites. The PCR protocol consisted of an initial denaturation at 98°C for 30 s, followed by 35 cycles of 98°C for 10 s, 58°C for 15 s and 72°C for 45 s, with a final extension at 72°C for 7 min. The PCR product was digested using *NdeI* and *XhoI* restriction enzymes (Thermo Fisher Scientific) and subsequently cloned into the pET30b vector using the *T4 ligase* enzyme (Thermo Fisher Scientific), according to the manufacturer's protocol. The pET30b plasmid introduces a 6xHis-tag at the C-terminal of the protein, facilitating downstream purification while maintaining the integrity of the BcSOD1 sequence. The resulting recombinant plasmid, pET30b-BcSOD1, was propagated and maintained in *E. coli* DH5α and confirmed by PCR, digestion and sequencing. For protein expression, the vector was introduced into *E. coli* BL21-CodonPlus-RIL by heat shock, using the protocol described by Mandel and Higa (1970).

4.3.2 | BcSOD1 Protein Expression and Purification

For in vitro production of the BcSOD1 protein, the *E. coli* strain BL21-CodonPlus-RIL, carrying the pET30b-BcSOD1 expression vector, was used. To achieve this, *E. coli* cells were cultured in LB medium containing 50 μg mL^{-1} kanamycin at 37°C. Once the cultures reached an optical density ($OD_{600\,nm}$) of 0.4, protein expression was induced with 0.5 mM IPTG (isopropyl-β-D-thiogalactopyranoside; Sigma-Aldrich). The cultures were incubated overnight at 16°C in an orbital shaker set at 80 rpm. After the incubation, cells were harvested by centrifugation at 8000 × *g* for 5 min at 4°C, and the resulting cell pellet was stored at −80°C overnight. Purification of the soluble BcSOD1 protein was performed using Protino Ni-TED 2000 Packed Columns (Macherey-Nagel GmbH & Co. KG, Düren, DE), which exploit the 6xHis-tag for affinity purification. The eluates were desalted using Sephadex G-25 in PD-10 desalting columns (GE Healthcare Technology Inc., Chicago, US) in 0.1 M sodium phosphate buffer (pH 7.8). The purified protein was verified using Mini-PROTEAN TGX (Bio-Rad, Hercules, US) and visualised in a GelDoc XR+ System (Bio-Rad). Finally, the protein concentration was estimated by the Protein Concentration Calculator website (https://www.aatbio.com/tools/calculate-protein-concentration) using the absorbance value at 280 nm, the extinction coefficient and the molecular weight of the protein, which was determined by the Expasy webserver (https://www.expasy.org/).

4.3.3 | Superoxide Dismutase (SOD) Activity Assay

To validate the activity of the heterologous-expressed BcSOD1 protein prior to aptamer selection, a cytochrome c reduction inhibition assay was performed, based on the method of McCord and Fridovich (1969) with slight modifications. For the assay, increasing concentrations of purified BcSOD1 (0.05, 0.1, 0.25, 0.5, 1, 2.5 and 5 μg mL^{-1}) were tested using a xanthine oxidase (XOD) solution (125 μg mL^{-1}; Sigma-Aldrich) and a reaction cocktail containing xanthine (0.108 mM; Sigma-Aldrich), cytochrome c (1.1 mM; Sigma-Aldrich) and EDTA (10.7 mM; Sigma-Aldrich), all prepared in potassium phosphate buffer (216 mM, pH 7.8). The reaction was monitored spectrophotometrically at 550 nm using a S-22 UV/Vis spectrophotometer (Boeco). The fastest linear velocity of absorbance change (ΔA) was recorded over 1 min under an uninhibited system (with XOD and reaction cocktail), which served as the baseline (negative) control. ΔA was determined at 550 nm ($\Delta A_{550\,nm}$) for each minute during 5 min. Moreover, the fastest $\Delta A_{550\,nm}$ of an inhibited system (4 μg mL^{-1} of commercial SOD -Sigma-Aldrich-, XOD and reaction cocktail) produced in the same time interval as in the uninhibited system was identified and used as a positive control. Subsequently, $\Delta A_{550\,nm}$ was measured in the same way using increasing concentrations of purified BcSOD1. Three independent replicates were performed, and the percentage inhibition of cytochrome c reduction was determined using the following formula:

$$\%\,\text{Inhibition} = \frac{\left(\Delta A_{550\,nm}/\text{min}\ \ \text{Uninhibited system} - \Delta A_{550\,nm}/\text{min}\ \ \text{Inhibited system}\right)}{\Delta A_{550\,nm}/\text{min}\ \ \text{Uninhibited system} - \Delta A_{550\,nm}/\text{min}\ \ \text{Blank}} \times 100$$

The assay was repeated to evaluate the effect of the selected aptamers on BcSOD1 activity. For this, $\Delta A_{550\,nm}$ was measured with increasing concentrations of aptamers (0.1, 1, 1, 10 and 100 nM, chosen from their Kd), pre-incubated with purified BcSOD1 (5 μg mL^{-1}) for 1, 6 and 24 h at 25°C under constant agitation (200 rpm). The percentage inhibition caused by the aptamers was calculated using the same formula, normalised to a fully inhibited system.

4.4 | Aptamer Selection Method and Synthesis

To obtain aptamers for purified BcSOD1, an in vitro process called SELEX (Figure S1) was conducted. DNA aptamers were selected through repetitive rounds of incubation, binding, partitioning and amplification steps using a random library of ssDNA (RDN40), which contained a central random region of 40 nucleotides flanked by two conserved 18-nucleotide regions at each end. A total of nine selection rounds were performed to obtain specific aptamers.

After rounds 3, 6 and 9 of SELEX, an ELONA was performed to monitor population enrichment and measure the affinity of each aptamer for its target protein. After round 9, the DNA pool was amplified by PCR, cloned, and the affinity of each individual aptamer candidate for the BcSOD1 target was tested by ELONA. The aptamers with the highest target protein affinity were sequenced, and the affinity of each chain for the

target was analysed by ELONA. Two aptamer candidates were selected, SOD9.14F (5′-GCGGATGAAGACTGGTGTCGGGGAGGGTGGGAGGGGGAGGTAGGTCGGGGTATGATCGGCCCTAAATACGAGCAAC-3′) and SOD9.26F (5′-GCGGATGAAGACTGGTGTGGTTGGGGGTCTGGCGGGGGGTGGGGAGGGCTGCGGGTGTGCCCTAAATACGAGCAAC-3′). Their equilibrium binding constant (Kd) values were determined, along with their secondary structures, using the RNAfold tool (Gruber et al. 2008) which calculated the minimum free energy based on DNA-specific parameters, allowing the understanding of potential base-pairing patterns and overall DNA conformation. Furthermore, these secondary structures were converted into a three-dimensional model using the 3dRNA/DNA tool (Zhang et al. 2024). This step generated detailed 3D representations of the DNA molecule's spatial arrangements.

4.5 | Molecular Modelling of the BcSOD1–Aptamer Binding

To understand how the aptamers bind to BcSOD1 but also to another *B. cinerea* SODs and to tomato SOD1 homologue, molecular modelling assays were conducted. First, the 3D structure of BcSOD1, BcSOD2, BcSOD3, BcSOD4 and *S. lycopersicum* SOD1 was obtained from AlphaFold Protein Structure Database (AFDB; Varadi et al. 2024), showing all of them a very high confidence structure (pLDDT >90). Next, the 3D structures of both DNA and protein molecules were prepared for in silico binding analysis using Autodock tools (Morris et al. 1998). This preparation involved three key steps: adding hydrogen atoms, merging nonpolar hydrogens and assigning Kolman charges to ensure accurate molecular representations for atomic interactions. Finally, the in silico docking analysis for BcSOD1, BcSOD2 and *S. lycopersicum* SOD1 was performed using HDOCK (Yan et al. 2017) a macromolecular docking tool. This simulated the interaction between the DNA aptamer (as the ligand) and the protein (as the receptor) to predict potential binding sites and molecular conformations. The final docking images were visualised with Pymol software.

4.6 | Aptamer Location

To study the in vitro location of the aptamers bound to BcSOD1, both aptamers were labelled with 5′-fluorescein (Sigma-Aldrich). Subsequently, a *B. cinerea* germination assay was carried out following the method of Hamby et al. (2020) with minor modifications. For this purpose, the fluorescein-labelled aptamers were diluted in phosphate-buffered saline (PBS; Na_2HPO_4 8.1 mM, KH_2PO_4 1.5 mM, NaCl 138 mM and KCl 3 mM) containing 1 mM $MgCl_2$. The aptamers were denatured for 10 min at 95°C and cooled for 10 min on ice to acquire their proper structure. Next, 5 μL of the fluorescein-labelled aptamers were applied to a glass microscope slide along with 5 μL of the *B. cinerea* conidial suspension (1×10^5 conidia mL^{-1}) in 2% water-agar media. Both the reference strain *B. cinerea* B05.10 and the Δ*Bcsod1* mutant were used in parallel. As negative controls, Milli-Q sterile water and the unspecific 38× (AG) control aptamer Ap.AGA (kindly provided by Dr. Víctor González, Aptamer Laboratory, Instituto Ramón y Cajal, Madrid; Rodriguez et al. 2016; García-Recio et al. 2016; de Arriba et al. 2022) were included. The slides were incubated at room temperature in the dark for 9 h. Milli-Q sterile water and unlabelled aptamers were used as negative controls. Before observation, the growing mycelium was treated with 75 U micrococcal nuclease (MNase) (Thermo Fisher Scientific) at 37°C for 30 min. The results were visualised using a laser scanning microscope (Zeiss LSM880, Zeiss Group, Oberkochen, DE).

4.7 | Sensitivity Assays of *B. cinerea* to Aptamers

4.7.1 | Effect on Conidia Germination

The effect of aptamers SOD9.14F and SOD9.26F on *B. cinerea* conidia germination was assessed through an in vitro assay using 12-well plates. A *B. cinerea* conidial suspension (1×10^5 conidia mL^{-1}) was mixed with different aptamer concentrations (50, 100 and 200 μM) and plated on 2% water-agar media. The assay was conducted using both the wild-type strain *B. cinerea* B05.10 and the Δ*Bcsod1* mutant to compare responses in the presence or absence of the target protein. Sterile Milli-Q water and the control DNA aptamer Ap.AGA were included as negative controls, while the commercial fungicide Geoxe (fludioxonil, Syngenta Crop Protection, Basel, CH) was used as a positive control. Plates were incubated at 23°C under a 16 h light/8 h dark photoperiod. The germination rate was analysed after 9 h of incubation using light microscopy and a Leica DM2500 microscope camera (Leica Microsystems, Wetzlar, DE). Images were processed with LAS-AF software LCS Lite (Leica Microsystems).

4.7.2 | Detached-Leaf Infection Assay

To evaluate the efficacy of the two aptamers against *B. cinerea*, a tomato detached-leaf infection assay was performed as described by Leisen et al. (2022), with minor modifications. For this purpose, different concentrations of the aptamer solutions were prepared in sterile distilled water and sprayed onto the surfaces of detached tomato leaves (from 3 weeks old plants). The leaves were placed on a Petri dish with water-agar media (0.5%) and, when dried, PDA discs (5 mm diameter and 2 mm thickness), pre-inoculated with 10 μL of *B. cinerea* B05.10 conidial suspension (1×10^4 conidia mL^{-1}), were placed onto them. The leaves were maintained at 23°C with 100% humidity under a 16 h light/8 h dark photoperiod for 72 h. Sterile distilled water and Geoxe (fludioxonil at a field dose of 1000 μM) were used as negative and positive controls, respectively. Lesions were photographed 72 h post-inoculation (hpi), and necrotic areas were quantified using ImageJ software.

In addition, to evaluate the potential immune-priming effect of exogenous DNA, a comparative assay was performed using the non-specific control aptamer Ap.AGA at 50 μM (same concentration used in transcriptomic analysis), sterile distilled water and the specific aptamer SOD9.26F at 50 μM. The assay conditions and result evaluation (incubation, imaging and necrosis quantification) were the same as described above.

4.7.3 | Fruit Infection Assay

To determine the effect of aptamer application on *B. cinerea* development in fruits, a fruit infection assay was carried out

using apple slices. Solutions containing 200 μM of aptamers were prepared in sterile distilled water and sprayed to the cut surfaces of apples. The treated surfaces were then placed in a container with moistened filter paper and inoculated with 10 μL of *B. cinerea* B05.10 conidial suspension (1×10^4 conidia mL^{-1}). The fruits were incubated at 23°C with 100% humidity under a 16 h light/8 h dark photoperiod. Sterile distilled water and Geoxe (fludioxonil at field dose 1000 μM) were included as negative and positive controls, respectively. The development of lesions and disease symptoms was assessed 4 days post-inoculation (dpi) using ImageJ software to calculate necrotic areas.

4.8 | Fungal Biomass Analysis

The molecular quantification of *B. cinerea* biomass was performed using qPCR. The primers used for this analysis were designed using the Primer3 software (Koressaar and Remm 2007; Thornton and Basu 2011) (Table S1). The molecular estimation of *B. cinerea* biomass was carried out by qPCR at 72 hpi from *B. cinerea* B05.10-infected tomato leaves. For this, the *B. cinerea* actin gene *BcactA* (XM_024697950.1) and the tomato actin gene *Slactin-51* (NM_001321306.1) were quantified, and the *B. cinerea*/*S. lycopersicum* genomic DNA ratio was calculated. The assay was carried out in a CFX Connect Real-Time PCR detection system (Bio-Rad) with SsoFast EvaGreen Supermix (Bio-Rad). The protocol included an enzyme activation step at 95°C for 30 s, followed by 40 cycles at 95°C for 5 s and 59°C for 5 s, and measuring individual amplification by a particular peak in the dissociation melting curve (from 55°C to 95°C in 0.5°C steps every 5 s). All reactions were performed in triplicate, and data were processed with CFX Manager Software (Bio-Rad).

4.9 | RNA-Seq Analysis

To better understand the effect of aptamer application on both *B. cinerea* and tomato plants, RNA-seq analyses were conducted. Separate experiments were conducted to evaluate gene expression changes following the application of the SOD9.26F aptamer to the fungus exposed to oxidative stress and to tomato plants.

For *B. cinerea* B05.10 strain, prior to RNA-seq analysis, the expression of *Bcsod1* gene (XM_001560480.2) was monitored at 0, 3, 6, 9, 12 and 24 h under oxidative stress. Stress was induced by adding 7.5 mM of paraquat (methyl viologen, Sigma-Aldrich), and expression was analysed using RT-qPCR using the same conditions described above and the primers described in Table S1. Subsequently, *B. cinerea* B05.10 was incubated in PDB at 25°C and 130 rpm for 72 h in the dark and supplemented with 7.5 mM of paraquat and 50 μM of aptamer SOD9.26F, incubating for 6 h. A negative control group without aptamer was also included. After incubation, the fungal mycelium was collected by centrifugation at 8000 × *g* and 4°C for 5 min, frozen in liquid nitrogen and stored at −80°C until RNA extraction.

For tomato, detached leaves (3-week-old plants) were sprayed with 50 μM of aptamer SOD9.26F or the control Ap.AGA aptamer and incubated for 72 h under the conditions described previously. A negative control group was also included. After incubation, leaves were collected, frozen in liquid nitrogen and stored at −80°C until RNA extraction. Each treatment tested included three biological replicates.

The frozen *B. cinerea* mycelium and tomato leaves were ground in liquid nitrogen with a mortar and pestle. Total RNA was extracted using TRI Reagent (Sigma-Aldrich) following the manufacturer's instructions. RNA quality and concentration were assessed using a Bioanalyzer 2100 system (Agilent Technologies, Santa Clara, US) and a Qubit 3.0 Fluorometer (Thermo Fisher Scientific). A total of 1 μg of RNA was used to prepare cDNA libraries using an Illumina Stranded mRNA Sample Preparation Kit (Illumina, San Diego, US) according to the manufacturer's guidelines. Finally, the cDNA libraries were sequenced using the Illumina NextSeq 550 and NovaSeq 6000 systems (Illumina), with a paired-end strategy. High-quality clean reads were mapped to the *B. cinerea* B05.10 or *S. lycopersicum* reference genomes (GenBank assembly name: GCA_000143535.4 and GCA_036512215.2, respectively) using the Rsubread software (Liao et al. 2019). Differential gene expression analysis was performed with DEGSeq2 R package (Love et al. 2014). For this purpose, raw reads were normalised using its median-of-ratios procedures: for each gene, we computed the geometric mean across samples, divided the count of each sample by this mean to derive gene-wise ratios, and obtained sample-specific size factors as the median of these ratios. After that, the differentially expressed genes (DEGs) were calculated between the three biological replicates of each treatment, with a p-adjust < 0.05 and values of $\log_2$ Fold Change (FC) < -1 or > 1. Functional enrichment of DEGs was performed using DAVID software (Sherman et al. 2022) based on the background annotations of *B. cinerea* and tomato.

4.10 | Statistical Analysis

For the statistical analyses carried out in this study, the GraphPad Prism software was used. Two-way ANOVA, followed by Fisher's least significant difference (LSD) test was carried out to compare the data obtained in aptamer inhibition assays, conidia germination rates and fungal biomass determined by qPCR.

Author Contributions

D.F.-O., Á.P. and A.L.-L. designed and planned the experiments. A.L.-L., Y.M. and A.V.-F. performed the experiments and analysed the data. M.E.M. and V.M.G. carried out aptamer synthesis. Á.P. and L.J.-C. performed RNA-Seq analyses. A.L.-L., Á.P. and D.F.-O. wrote the manuscript draft. A.L.-L., Á.P., A.V., A.P.-G. and D.F.-O. revised the manuscript. A.P.-G. and D.F.-O. supervised the study and obtained the funds. All authors read the manuscript and approved its content.

Acknowledgements

We sincerely thank Professor Matthias Hahn (University of Kaiserslautern-Landau) for kindly providing the Δ*Bcsod1* mutant used in this study. We also kindly acknowledge the excellent technical support provided by Virginia Mota. This work has been funded by: AYUDAS A LA I+D+i, EN EL ÁMBITO DEL PLAN ANDALUZ DE INVESTIGACIÓN, DESARROLLO E INNOVACIÓN (PAIDI 2020). Project code: PY20_00048.

Conflicts of Interest

The authors declare no conflicts of interest.

Data Availability Statement

The data that support the findings of this study are openly available in Universidad de Málaga/CBUA at https://riuma.uma.es/xmlui/.

References

Ali, O., A. Ramsubhag, and J. Jayaraman. 2022. "Transcriptome-Wide Modulation by *Sargassum vulgare* and *Acanthophora spicifera* Extracts Results in a Prime-Triggered Plant Signalling Cascade in Tomato and Sweet Pepper." *AoB Plants* 14: plac046.

Almagro-Armenteros, J. J., C. K. Sønderby, S. K. Sønderby, H. Nielsen, and O. Winther. 2017. "DeepLoc: Prediction of Protein Subcellular Localization Using Deep Learning." *Bioinformatics* 33: 3387–3395.

Amaya-González, S., N. de-Los-Santos-Álvarez, A. J. Miranda-Ordieres, and M. J. Lobo-Castañón. 2014. "Aptamer Binding to Celiac Disease-Triggering Hydrophobic Proteins: A Sensitive Gluten Detection Approach." *Analytical Chemistry* 86: 2733–2739.

Amselem, J., C. A. Cuomo, J. A. L. van Kan, et al. 2011. "Genomic Analysis of the Necrotrophic Fungal Pathogens *Sclerotinia sclerotiorum* and *Botrytis cinerea*." *PLoS Genetics* 7: e1002230.

Banerjee, J. 2010. "Antibodies Are Challenged." *Indian Journal of Medical Sciences* 64: 144–147.

Choquer, M., E. Fournier, C. Kunz, et al. 2007. "*Botrytis cinerea* Virulence Factors: New Insights Into a Necrotrophic and Polyphageous Pathogen." *FEMS Microbiology Letters* 277: 1–10.

Cruz-Garcia, D., N. Brouwers, J. M. Duran, G. Mora, A. J. Curwin, and V. Malhotra. 2017. "A Diacidic Motif Determines Unconventional Secretion of Wild-Type and ALS-Linked Mutant SOD1." *Journal of Cell Biology* 216: 2691–2700.

De Angelis, G., G. Simonetti, L. Chronopoulou, et al. 2022. "A Novel Approach to Control *Botrytis cinerea* Fungal Infections: Uptake and Biological Activity of Antifungals Encapsulated in Nanoparticle Based Vectors." *Scientific Reports* 12: 7989.

de Arriba, M. D. C., G. Fernández, E. Chacón-Solano, et al. 2022. "FPR2 DNA Aptamers for Targeted Therapy of Wound Repair." *Journal of Investigative Dermatology* 142: 2238–2248.

de Gara, L., M. C. de Pinto, and F. Tommasi. 2003. "The Antioxidant Systems Vis a Vis Reactive Oxygen Species During Plant–Pathogen Interaction." *Plant Physiology and Biochemistry* 41: 863–870.

Dean, R., J. A. L. Van Kan, Z. A. Pretorius, et al. 2012. "The Top 10 Fungal Pathogens in Molecular Plant Pathology." *Molecular Plant Pathology* 13: 414–430.

Doehlemann, G., B. Ökmen, W. Zhu, and A. Sharon. 2017. "Plant Pathogenic Fungi." In *The Fungal Kingdom*, edited by J. Heitman, B. J. Howlett, P. W. Crous, E. H. Stukenbrock, T. Y. James, and N. A. R. Gow, 701–726. American Society for Microbiology.

Duanis-Assaf, D., O. Galsurker, O. Davydov, et al. 2022. "Double-Stranded RNA Targeting Fungal Ergosterol Biosynthesis Pathway Controls *Botrytis cinerea* and Postharvest Grey Mould." *Plant Biotechnology Journal* 20: 226–237.

Ellington, A. D., and J. W. Szostak. 1990. "*In Vitro* Selection of RNA Molecules That Bind Specific Ligands." *Nature* 346: 818–822.

Fernández-Ortuño, D., A. Grabke, X. Li, and G. Schnabel. 2015. "Independent Emergence of Resistance to Seven Chemical Classes of Fungicides in *Botrytis cinerea*." *Phytopathology* 105: 424–432.

Fernández-Ortuño, D., A. Pérez-García, M. Chamorro, E. de la Peña, A. de Vicente, and J. A. Torés. 2017. "Resistance to the SDHI Fungicides Boscalid, Fluopyram, Fluxapyroxad, and Penthiopyrad in *Botrytis cinerea* From Commercial Strawberry Fields in Spain." *Plant Disease* 101: 1306–1313.

Ferrusquía-Jiménez, N. I., G. Chandrakasan, I. Torres-Pacheco, E. Rico-Garcia, A. A. Feregrino-Perez, and R. G. Guevara-González. 2021. "Extracellular DNA: A Relevant Plant Damage-Associated Molecular Pattern (DAMP) for Crop Protection Against Pests—A Review." *Journal of Plant Growth Regulation* 40: 451–463.

Fridovich, I. 1981. "Superoxide Radical and Superoxide Dismutases." In *Oxygen and Living Processes. Topics in Environmental Physiology and Medicine*, edited by D. L. Gilbert, 250–272. Springer.

García-Recio, E. M., C. Pinto-Díez, M. I. Pérez-Morgado, et al. 2016. "Characterization of MNK1b DNA Aptamers That Inhibit Proliferation in MDA-MB231 Breast Cancer Cells." *Molecular Therapy—Nucleic Acids* 5: e275.

Ghe, A. M., C. Stefanelli, P. Tsintiki, and G. Veschi. 1985. "Influence of Some Metal Ions on Oxidation of NADH and on Formation of the Superoxide Anion Radical (O_2–), During Enzymatic Catalysis by EC 1.2. 3.2 Xanthine Oxidase." *Talanta* 32: 359–362.

Gopinath, S. C. B., K. H. Hayashi, and P. K. R. Kumar. 2012. "Aptamer That Binds to the gD Protein of Herpes Simplex Virus 1 and Efficiently Inhibits Viral Entry." *Journal of Virology* 86: 6732–6744.

Govrin, E. M., and A. Levine. 2000. "The Hypersensitive Response Facilitates Plant Infection by the Necrotrophic Pathogen *Botrytis cinerea*." *Current Biology* 10: 751–757.

Gruber, A. R., R. Lorenz, S. H. Bernhart, R. Neuböck, and I. L. Hofacker. 2008. "The Vienna RNA Websuite." *Nucleic Acids Research* 36: W70–W74.

Hamby, R., M. Wang, L. Qiao, and H. Jin. 2020. "Synthesizing Fluorescently Labeled dsRNAs and sRNAs to Visualize Fungal RNA Uptake." In *RNA Tagging. Methods in Molecular Biology*, edited by M. Heinlein, 215–225. Humana.

Hamilton, A. J., M. D. Holdom, and L. Jeavons. 1996. "Expression of the Cu,Zn Superoxide Dismutases of *Aspergillus fumigatus* as Determined by Immunochemistry and Immunoelectron Microscopy." *FEMS Immunology and Medical Microbiology* 14: 95–102.

Han, S. R., J. Yu, and S. W. Lee. 2014. "*In Vitro* Selection of RNA Aptamers That Selectively Bind Danofloxacin." *Biochemical and Biophysical Research Communications* 448: 397–402.

Harper, L. A., S. Paton, B. Hall, S. McKay, R. P. Oliver, and F. J. Lopez-Ruiz. 2021. "Fungicide Resistance Characterized Across Seven Modes of Action in *Botrytis cinerea* Isolated From Australian Vineyards." *Pest Management Science* 78: 1326–1340.

He, J., Y. Liu, F. de Mingtao, and X. Liu. 2011. "Isolation and Identification of the DNA Aptamer Target to Acetamiprid." *Journal of Agricultural and Food Chemistry* 59: 1582–1586.

Hernández, Y., L. K. Lagos, and B. C. Galarreta. 2020. "Development of a Label-Free-SERS Gold Nanoaptasensor for the Accessible Determination of Ochratoxin A." *Sensing and Bio-Sensing Research* 28: 100331.

Huang, Y., C. Huang, J. Chen, et al. 2024. "Inhibition of SARS-CoV-2 Replication by a ssDNA Aptamer Targeting the Nucleocapsid Protein." *Microbiology Spectrum* 12: e03410-23.

Islam, M. T., Z. Davis, L. Chen, et al. 2021. "Minicell-Based Fungal RNAi Delivery for Sustainable Crop Protection." *Microbial Biotechnology* 14: 1847–1856.

Kaleh, A. M., P. Singh, K. O. Chua, and J. A. Harikrishna. 2024. "Modulation of Plant Transcription Factors and Priming of Stress Tolerance by Plant Growth-Promoting Bacteria: A Systematic Review." *Annals of Botany* 135: mcae166.

Kim, Y. K., and C. L. Xiao. 2011. "Stability and Fitness of Pyraclostrobin- and Boscalid-Resistant Phenotypes in Field Strains of *Botrytis cinerea* From Apple." *Phytopathology* 101: 1385–1391.

Koressaar, T., and M. Remm. 2007. "Enhancements and Modifications of Primer Design Program Primer3." *Bioinformatics* 23: 1289–1291.

Ku, T. H., T. Zhang, H. Luo, et al. 2015. "Nucleic Acid Aptamers: An Emerging Tool for Biotechnology and Biomedical Sensing." *Sensors (Basel)* 15: 16281–16313.

Leisen, T., F. Bietz, J. Werner, et al. 2020. "CRISPR/Cas With Ribonucleoprotein Complexes and Transiently Selected Telomere Vectors Allows Highly Efficient Marker-Free and Multiple Genome Editing in *Botrytis cinerea*." *PLoS Pathogens* 16: e1008326.

Leisen, T., J. Werner, P. Pattar, et al. 2022. "Multiple Knockout Mutants Reveal a High Redundancy of Phytotoxic Compounds Contributing to Necrotrophic Pathogenesis of *Botrytis cinerea*." *PLoS Pathogens* 18: e1010367.

Liao, Y., G. K. Smyth, and W. Shi. 2019. "The R Package Rsubread Is Easier, Faster, Cheaper and Better for Alignment and Quantification of RNA Sequencing Reads." *Nucleic Acids Research* 47: e47.

Lopes, U. P., L. Zambolim, N. P. Capobiango, N. A. O. Gracia, and R. L. Freitas-Lopes. 2017. "Resistance of *Botrytis cinerea* to Fungicides Controlling Gray Mold on Strawberry in Brazil." *Bragantia* 76: 266–272.

López-Cruz, J., O. Crespo-Salvador, E. Fernández-Crespo, P. García-Agustín, and C. González-Bosch. 2017. "Absence of Cu–Zn Superoxide Dismutase BCSOD1 Reduces *Botrytis cinerea* Virulence in Arabidopsis and Tomato Plants, Revealing Interplay Among Reactive Oxygen Species, Callose and Signalling Pathways." *Molecular Plant Pathology* 18: 16–31.

Love, M. I., W. Huber, and S. Anders. 2014. "Moderated Estimation of Fold Change and Dispersion for RNA-Seq Data With DESeq2." *Genome Biology* 15: 550.

Mahlknecht, G., R. Maron, M. Mancini, B. Schechter, M. Sela, and Y. Yarden. 2013. "Aptamer to ErbB-2/HER2 Enhances Degradation of the Target and Inhibits Tumorigenic Growth." *Proceedings of the National Academy of Sciences of the United States of America* 110: 8170–8175.

Mandel, M., and A. Higa. 1970. "Calcium-Dependent Bacteriophage DNA Infection." *Journal of Molecular Biology* 53: 159–162.

McCord, J. M., and I. Fridovich. 1969. "Superoxide Dismutase: An Enzymic Function for Erythrocuprein (Hemocuprein)." *Journal of Biological Chemistry* 244: 6049–6055.

Missailidis, S., and A. Hardy. 2009. "Aptamers as Inhibitors of Target Proteins." *Expert Opinion on Therapeutic Patents* 19: 1073–1082.

Moore, S., O. M. H. de Vries, and P. Tudzynski. 2002. "The Major Cu, Zn SOD of the Phytopathogen *Claviceps purpurea* Is Not Essential for Pathogenicity." *Molecular Plant Pathology* 3: 9–22.

Morris, G. M., D. S. Goodsell, R. S. Halliday, et al. 1998. "Automated Docking Using a Lamarckian Genetic Algorithm and Empirical Binding Free Energy Function." *Journal of Computational Chemistry* 19: 1639–1662.

Nair, A. U., D. P. N. Bhukya, R. Sunkar, S. Chavali, and A. D. Allu. 2022. "Molecular Basis of Priming-Induced Acquired Tolerance to Multiple Abiotic Stresses in Plants." *Journal of Experimental Botany* 73: 3355–3371.

Nguyen, B. H., L. D. Tran, Q. P. Do, H. L. Nguyen, N. H. Tran, and P. X. Nguyen. 2013. "Label-Free Detection of Aflatoxin M1 With Electrochemical Fe_3O_4/Polyaniline-Based Aptasensor." *Materials Science and Engineering: C* 33: 2229–2234.

Niehl, A., I. Wyrsch, T. Boller, and M. Heinlein. 2016. "Double-Stranded RNAs Induce a Pattern-Triggered Immune Signaling Pathway in Plants." *New Phytologist* 211: 1008–1019.

Pang, S., T. P. Labuza, and L. He. 2014. "Development of a Single Aptamer-Based Surface Enhanced Raman Scattering Method for Rapid Detection of Multiple Pesticides." *Analyst* 139: 1895–1901.

Patel, R. M., J. A. L. Van Kan, A. M. Bailey, and G. D. Foster. 2008. "RNA-Mediated Gene Silencing of Superoxide Dismutase (*bcsod1*) in *Botrytis cinerea*." *Phytopathology* 98: 1334–1339.

Petrasch, S., S. J. Knapp, J. A. L. van Kan, and B. Blanco-Ulate. 2019. "Grey Mould of Strawberry, a Devastating Disease Caused by the Ubiquitous Necrotrophic Fungal Pathogen *Botrytis cinerea*." *Molecular Plant Pathology* 20: 877–892.

Pierleoni, A., P. L. Martelli, and R. Casadio. 2008. "PredGPI: A GPI-Anchor Predictor." *BMC Bioinformatics* 9: 1–11.

Plante, S., V. Normant, K. M. Ramos-Torres, and S. Labbé. 2017. "Cell-Surface Copper Transporters and Superoxide Dismutase 1 Are Essential for Outgrowth During Fungal Spore Germination." *Journal of Biological Chemistry* 292: 11896–11914.

Proske, D., S. Gilch, F. Wopfner, H. M. Schätzl, E. L. Winnacker, and M. Famulok. 2002. "Prion-Protein-Specific Aptamer Reduces PrP^{Sc} Formation." *Chembiochem* 3: 717–725.

Qiao, L., J. Niño-Sánchez, R. Hamby, et al. 2023. "Artificial Nanovesicles for dsRNA Delivery in Spray-Induced Gene Silencing for Crop Protection." *Plant Biotechnology Journal* 21: 854–865.

Qin, G., J. Liu, B. Cao, B. Li, and S. Tian. 2011. "Hydrogen Peroxide Acts on Sensitive Mitochondrial Proteins to Induce Death of a Fungal Pathogen Revealed by Proteomic Analysis." *PLoS One* 6: e21945.

Rodriguez, P., M. I. Pérez-Morgado, V. M. Gonzalez, M. E. Martín, and A. Nieto. 2016. "Inhibition of Influenza Virus Replication by DNA Aptamers Targeting a Cellular Component of Translation Initiation." *Molecular Therapy—Nucleic Acids* 5: e308.

Rolke, Y., S. Liu, T. Quidde, et al. 2004. "Functional Analysis of H_2O_2-Generating Systems in *Botrytis cinerea*: The Major Cu-Zn-Superoxide Dismutase (BCSOD1) Contributes to Virulence on French Bean, Whereas a Glucose Oxidase (BCGOD1) is Dispensable." *Molecular Plant Pathology* 5: 17–27.

Sang, C., W. Ren, J. Wang, et al. 2018. "Detection and Fitness Comparison of Target-Based Highly Fludioxonil-Resistant Strains of *Botrytis cinerea* From Strawberry and Cucumber in China." *Pesticide Biochemistry and Physiology* 147: 110–118.

Sellés-Vidal, L., C. Kelly, P. M. Mordaka, and J. T. Heap. 2018. "Review of NAD(P)H-Dependent Oxidoreductases: Properties, Engineering and Application." *Biochimica et Biophysica Acta, Proteins and Proteomics* 1866: 327–347.

Serrano-Jamaica, L. M., E. Villordo-Pineda, M. M. González-Chavira, R. G. Guevara-González, and G. Medina-Ramos. 2021. "Effect of Fragmented DNA From Plant Pathogens on the Protection Against Wilt and Root Rot of *Capsicum annuum* L. Plants." *Frontiers in Plant Science* 11: 581891.

Sherman, B. T., M. Hao, J. Qiu, et al. 2022. "DAVID: A Web Server for Functional Enrichment Analysis and Functional Annotation of Gene Lists (2021 Update)." *Nucleic Acids Research* 50: W216–W221.

Shi, H., X. He, K. Wang, et al. 2011. "Activatable Aptamer Probe for Contrast-Enhanced *In Vivo* Cancer Imaging Based on Cell Membrane Protein-Triggered Conformation Alteration." *Proceedings of the National Academy of Sciences of the United States of America* 108: 3900–3905.

Siegmund, U., and A. Viefhues. 2016. "Reactive Oxygen Species in the *Botrytis*-Host Interaction." In *Botrytis – The Fungus, the Pathogen and Its Management in Agricultural Systems*, edited by S. Fillinger and Y. Elad, 269–289. Springer International Publishing.

Sillitoe, I., N. Bordin, N. Dawson, et al. 2021. "CATH: Increased Structural Coverage of Functional Space." *Nucleic Acids Research* 49: D266–D273.

Spada, M., C. Pugliesi, M. Fambrini, D. Palpacelli, and S. Pecchia. 2023. "Knockdown of *Bmp1* and *Pls1* Virulence Genes by Exogenous Application of RNAi-Inducing dsRNA in *Botrytis cinerea*." *International Journal of Molecular Sciences* 24: 4869.

Spada, M., C. Pugliesi, M. Fambrini, and S. Pecchia. 2021. "Silencing of the Slt2-Type MAP Kinase *Bmp3* in *Botrytis cinerea* by Application of Exogenous dsRNA Affects Fungal Growth and Virulence on *Lactuca sativa*." *International Journal of Molecular Sciences* 22: 5362.

Staats, M., and J. A. van Kan. 2012. "Genome Update of Botrytis Cinerea Strains B05. 10 and T4." *Eukaryotic Cell* 11: 1413–1414.

Thornton, B., and C. Basu. 2011. "Real-Time PCR (qPCR) Primer Design Using Free Online Software." *Biochemistry and Molecular Biology Education* 39: 145–154.

Tian, L., C. Huang, D. Zhang, et al. 2021. "Extracellular Superoxide Dismutase VdSOD5 Is Required for Virulence in *Verticillium dahliae*." *Journal of Integrative Agriculture* 20: 1858–1870.

Tian, L., J. Li, C. Huang, et al. 2021. "Cu/Zn Superoxide Dismutase (*VdSOD1*) Mediates Reactive Oxygen Species Detoxification and Modulates Virulence in *Verticillium dahliae*." *Molecular Plant Pathology* 22, no. 9: 1092–1108.

Trisolini, L., N. Gambacorta, R. Gorgoglione, et al. 2019. "FAD/NADH Dependent Oxidoreductases: From Different Amino Acid Sequences to Similar Protein Shapes for Playing an Ancient Function." *Journal of Clinical Medicine* 8: 2117.

Tuerk, C., and L. Gold. 1990. "Systematic Evolution of Ligands by Exponential Enrichment: RNA Ligands to Bacteriophage T4 DNA Polymerase." *Science* 249: 505–510.

Tzin, V., and G. Galili. 2010. "The Biosynthetic Pathways for Shikimate and Aromatic Amino Acids in *Arabidopsis thaliana*." *Arabidopsis Book* 8: e0132.

Van Kan, J. A. L., J. H. M. Stassen, A. Mosbach, et al. 2017. "A Gapless Genome Sequence of the Fungus *Botrytis cinerea*." *Molecular Plant Pathology* 18: 75–89.

Varadi, M., D. Bertoni, P. Magana, et al. 2024. "AlphaFold Protein Structure Database in 2024: Providing Structure Coverage for Over 214 Million Protein Sequences." *Nucleic Acids Research* 52: D368–D375.

Vega-Muñoz, I., A. Herrera-Estrella, O. Martínez-de la Vega, and M. Heil. 2023. "ATM and ATR, Two Central Players of the DNA Damage Response, Are Involved in the Induction of Systemic Acquired Resistance by Extracellular DNA, but Not the Plant Wound Response." *Frontiers in Immunology* 14: 1175786.

Veluchamy, S., B. Williams, K. Kim, and M. B. Dickman. 2012. "The CuZn Superoxide Dismutase From *Sclerotinia sclerotiorum* Is Involved With Oxidative Stress Tolerance, Virulence, and Oxalate Production." *Physiological and Molecular Plant Pathology* 78: 14–23.

Wang, C. H., C. P. Chang, and G. B. Lee. 2016. "Integrated Microfluidic Device Using a Single Universal Aptamer to Detect Multiple Types of Influenza Viruses." *Biosensors & Bioelectronics* 86: 247–254.

Wang, L., S. Lyu, G. Gu, and S. Bolten. 2020. "Selection of Aptamers Targeted to Food-Borne Pathogenic Bacteria *Vibrio parahaemolyticus*." *Food Science & Nutrition* 8: 3835–3842.

Wang, M., A. Weiberg, F. M. Lin, B. P. Thomma, H. D. Huang, and H. Jin. 2016. "Bidirectional Cross-Kingdom RNAi and Fungal Uptake of External RNAs Confer Plant Protection." *Nature Plants* 2: 1–10.

Wang, Q., A. Pokhrel, and J. J. Coleman. 2021. "The Extracellular Superoxide Dismutase Sod5 From *Fusarium oxysporum* Is Localized in Response to External Stimuli and Contributes to Fungal Pathogenicity." *Frontiers in Plant Science* 12: 608861.

Willi, J., P. Küpfer, D. Evéquoz, et al. 2018. "Oxidative Stress Damages rRNA Inside the Ribosome and Differentially Affects the Catalytic Center." *Nucleic Acids Research* 46: 1945–1957.

Williamson, B., B. Tudzynski, P. Tudzynski, and J. A. L. Van Kan. 2007. "*Botrytis cinerea*: The Cause of Grey Mould Disease." *Molecular Plant Pathology* 8: 561–580.

Yakushiji, S., Y. Ishiga, Y. Inagaki, K. Toyoda, T. Shiraishi, and Y. Ichinose. 2009. "Bacterial DNA Activates Immunity in *Arabidopsis thaliana*." *Journal of General Plant Pathology* 75: 227–234.

Yan, Y., D. Zhang, P. Zhou, B. Li, and S. Y. Huang. 2017. "HDOCK: A Web Server for Protein–Protein and Protein–DNA/RNA Docking Based on a Hybrid Strategy." *Nucleic Acids Research* 45: W365–W373.

Yao, S. H., Y. Guo, Y. Z. Wang, D. Zhang, L. Xu, and W. H. Tang. 2016. "A Cytoplasmic Cu-Zn Superoxide Dismutase SOD1 Contributes to Hyphal Growth and Virulence of *Fusarium graminearum*." *Fungal Genetics and Biology* 91: 32–42.

Youn, H. D., E. J. Kim, J. H. Roe, Y. C. Hah, and S. O. Kang. 1996. "A Novel Nickel-Containing Superoxide Dismutase From *Streptomyces* spp." *Biochemical Journal* 318: 889–896.

Zhang, Y., Y. Xiong, C. Yang, and Y. Xiao. 2024. "3dRNA/DNA: 3D Structure Prediction From RNA to DNA." *Journal of Molecular Biology* 436: 168742.

Zhang, Z., Y. Chen, B. Li, T. Chen, and S. Tian. 2020. "Reactive Oxygen Species: A Generalist in Regulating Development and Pathogenicity of Phytopathogenic Fungi." *Computational and Structural Biotechnology Journal* 18: 3344–3349.

Zhou, X., H. Gao, X. Zhang, et al. 2023. "Plant Extracellular Self-DNA Inhibits Growth and Induces Immunity via the Jasmonate Signaling Pathway." *Plant Physiology* 192: 2475–2491.

Zou, X., J. Wu, J. Gu, L. Shen, and L. Mao. 2019. "Application of Aptamers in Virus Detection and Antiviral Therapy." *Frontiers in Microbiology* 10: 1462.

Supporting Information

Additional supporting information can be found online in the Supporting Information section. **Appendix S1:** pbi70317-sup-0001-AppendixS1.docx. **TABLE S3:** pbi70317-sup-0002-TableS3.xlsx